Dalton
Transactions

Cite this: *Dalton Trans.*, 2012, **41**, 4517

www.rsc.org/dalton

PAPER

Synthesis and reactivity of molybdenum and tungsten bis(dinitrogen) complexes supported by diphosphine chelates containing pendant amines†

Charles J. Weiss,[a] Amy N. Groves,[a] Michael T. Mock,*[a] William G. Dougherty,[b] W. Scott Kassel,[b] Monte L. Helm,‡[a,c] Daniel L. DuBois[a] and R. Morris Bullock*[a]

Received 21st November 2011, Accepted 11th January 2012
DOI: 10.1039/c2dt12224c

Molybdenum and tungsten bis(dinitrogen) complexes of the formula $M(N_2)_2(PNP)_2$ (M = Mo and W) and $W(N_2)_2(dppe)(PNP)$, supported by diphosphine ligands containing a pendant amine of the formula $(CH_2PR_2)_2NR' = P^RN^{R'}P^R$ (R = Et, Ph; R′ = Me, Bn), have been prepared by Mg reduction of metal halides under an N_2 atmosphere. The complexes have been characterized by NMR and IR spectroscopy, X-ray crystallography, and cyclic voltammetry. Reactivity of the target Mo and W bis(dinitrogen) compounds with CO results in the formation of dicarbonyl complexes.

Introduction

The Haber–Bosch process is the industrial method for production of ammonia using hydrogen and nitrogen feedstocks.[1] Nitrogenase enzymes convert N_2 to NH_3 under ambient conditions.[2] In contrast, the energy-intensive industrial synthesis of NH_3, which includes the production of H_2 (by steam reforming of methane) and the reduction of N_2 at high temperatures and pressures, is estimated to account for approximately 1% of the global human energy consumption.[1b,3] The coordination of dinitrogen to a transition-metal center has been known for almost 50 years.[4] This discovery led to the development of coordination complexes and homogeneous catalysts that can facilitate the reduction of dinitrogen to ammonia under mild temperatures and pressures.[5]

Brønsted acid-mediated reduction of dinitrogen to ammonia at a single transition-metal center has been pursued as a more energy efficient route for ammonia production. The advantages are both in the milder temperatures and pressures required for N_2 reduction and bypassing the energy-intensive H_2 production by using a combination of protons and electrons. The pioneering research by Chatt, Hidai and coworkers[6] demonstrated that addition of strong acids to molybdenum and tungsten dinitrogen complexes, supported by monodentate or chelating phosphine ligands, produced a stoichiometric quantity of ammonia. Since this pioneering work, only two examples of catalytic production of ammonia have been reported. Schrock[5b–e] demonstrated NH_3 could be produced at a single metal center by a Mo(III) catalyst supported by a sterically demanding triamidoamine ligand, $[HIPTN_3N]^{3-} = \{3,5\text{-}(2,4,6\text{-}^iPr_3C_6H_2)_2C_6H_3NCH_2CH_2]_3N\}^{3-}$. Recently, a catalytic system was reported by the group of Nishibayashi using a Mo(0) catalyst $[Mo(L)(N_2)_2]_2(\mu\text{-}N_2)$, (L = 2,6-bis(di-*tert*-butyl-phosphinomethyl)pyridine) supported by a phosphine-based pincer ligand.[5a] These Mo complexes reduce N_2 catalytically upon addition of protons and electrons. The protons come from the weak acids, $[lutidinium][B(3,5\text{-}(CF_3)_2C_6H_3)_4$ and 2,6-lutidinium triflate, while the electrons are from a chemical reductant, decamethyl chromocene and cobaltocene, respectively.

Our group is interested in the preparation of molecular electrocatalysts that can be used to perform multi-proton, multi-electron transformations.[7] In our efforts, we implement proton relays, functional groups that are intended to facilitate the delivery of protons, into the second coordination sphere of the catalysts. For example, nickel complexes containing amine proton relays in the backbone of chelating diphosphine ligands have been shown to produce highly active electrocatalysts for the reduction of protons to H_2.[8] Our interest in designing electrocatalysts for applications such as reduction of O_2[9] and N_2[10] builds upon this concept.

The achievement of catalytic reduction of N_2 of metal-bound dinitrogen with the addition of protons and electrons described above, inspired us to investigate if "Chatt-type" dinitrogen complexes with group 6 metals, $(M(N_2)_2(P\text{–}P)_2$, P–P = diphosphine ligand, M = Mo and W), may benefit from adding proton relays, where incorporation of a pendant amine in the phosphine ligand backbone could assist with the delivery of protons to a metal-bound dinitrogen ligand. In a related report, Tuczek *et al.*[11] explored the coordination chemistry of Mo and W complexes bearing diphosphine ligands containing proton relays. The

---

[a] *Center for Molecular Electrocatalysis, Pacific Northwest National Laboratory, P.O. Box 999, Richland, Washington 99352, USA. E-mail: michael.mock@pnnl.gov, morris.bullock@pnnl.gov*
[b] *Department of Chemistry, Villanova University, Villanova, Pennsylvania 19085, USA*
[c] *Department of Chemistry, Fort Lewis College, Durango, Colorado 81301, USA*

† Electronic supplementary information (ESI) available: X-ray crystallographic data and experimentals, NMR and IR electrochemical data. CCDC reference numbers 854188–854202 and 863033. For ESI and crystallographic data in CIF or other electronic format see DOI: 10.1039/c2dt12224c

‡ Sabbatical visitor at PNNL, 2010–2011.

addition of 3 equiv. $HBF_4{\cdot}OEt_2$ to one such complex, *trans*-[Mo$(N_2)_2$(dppe)($pyNP_2$)], (dppe = 1,2-bis(diphenylphosphino)ethane; $pyNP_2$ = *N*,*N*-bis(diphenylphosphinomethyl)-2-aminopyridine) resulted in the isolation of *trans*-[MoF(NNH_2)(dppe)(pyN(H)P_2)][BF_4]$_2$, where protonation occurred at the pyridine nitrogen of the proton relay and at the dinitrogen ligand.[12]

Herein we report the synthesis and characterization of molybdenum bis(dinitrogen) complexes supported by two PNP diphosphine ligands, Mo$(N_2)_2$(PNP)$_2$; PNP = [($R_2PCH_2)_2$N(R′), R = Et, Ph; R′ = Me, Bn], and a series of tungsten bis(dinitrogen) complexes containing one or two PNP ligands, W$(N_2)_2$(dppe)(PNP) and W$(N_2)_2$(PNP)$_2$, respectively, and the analogues without pendant amines for comparison. These Mo– and W–N_2 complexes, which contain flexible[11,13] pendant amines in the second coordination sphere, were characterized by NMR and IR spectroscopy, cyclic voltammetry and structural characterization by X-ray crystallography. In addition, reactivity of the complexes with CO is described.

Results and discussion

Entry into PNP-supported molybdenum chemistry is sensitive to the nature of the Mo starting material. Efforts to prepare the targeted Mo$(N_2)_2$(PNP)$_2$ complexes by reported reductive synthetic routes[14] using starting materials such as $MoCl_5$, $MoCl_4(Et_2O)$, or $MoCl_3(THF)_3$ were unsuccessful.[15] These results are surprising, considering these starting materials are routinely used with non-pendant amine containing phosphines, such as the reductive synthesis of *trans*-[Mo$(N_2)_2$(dppe)$_2$][16] or [Mo$(N_2)_2(PMePh_2)_4$].[17] In our studies, $MoBr_3(THF)_3$ was used to prepare the target Mo$(N_2)_2$(PNP)$_2$ complexes by two methods: a direct reduction of $MoBr_3(THF)_3$ to Mo$(N_2)_2$(PNP)$_2$ or by the stepwise reduction of isolated $MoBr_2$(PNP)$_2$, Scheme 1.

The dibromide complexes, $MoBr_2$(PNP)$_2$ are prepared in THF by reducing $MoBr_3(THF)_3$ with Zn flakes in the presence of two equivalents of the desired PNP ligand. Isolated yields of the yellow or orange, paramagnetic $MoBr_2$(PNP)$_2$ complexes were found to be dependent upon the identity of the phosphorus substituents on the PNP ligand. The yield of isolable dibromide compounds, $MoBr_2(P^{Et}N^{Bn}P^{Et})_2$ (**1**) and $MoBr_2(P^{Et}N^{Me}P^{Et})_2$ (**2**), is low (21–29%), which is in part due to the formation of a blue–green molybdenum dimer, $[MoBr_2(P^{Et}N^{R}P^{Et})]_2$ (R = Bn and Me), isolated in 29% yield by diethyl ether extraction, and structurally characterized by X-ray diffraction, Fig. 1h (see ESI† for crystallographic metrics). Similar Mo dimers have been reported by Walton[18] and Cotton,[19] such as $[MoCl_2(dppe)]_2$,[19a] through the reaction of molybdenum halide salts (*e.g.*, $K_4Mo_2Cl_8$) and monodentate or chelating phosphines. Treatment of $[MoBr_2(P^{Et}N^{Bn}P^{Et})]_2$ with Mg powder does not yield a dinitrogen complex, suggesting it is not an intermediate in the reductive synthesis of the Mo(N_2) complexes (*vide infra*). In contrast to the synthesis of **1** and **2**, the preparation of dibromide complexes containing phenylphosphine-substituted ligands, $MoBr_2(P^{Ph}N^{Me}P^{Ph})_2$ (**3**) and $MoBr_2(P^{Ph}N^{Bn}P^{Ph})_2$ (**4**), proceeds smoothly with yields of 78–80%. All $MoBr_2$(PNP)$_2$ complexes are insoluble in ether or hexanes, and are sparingly soluble in dichloromethane and THF.

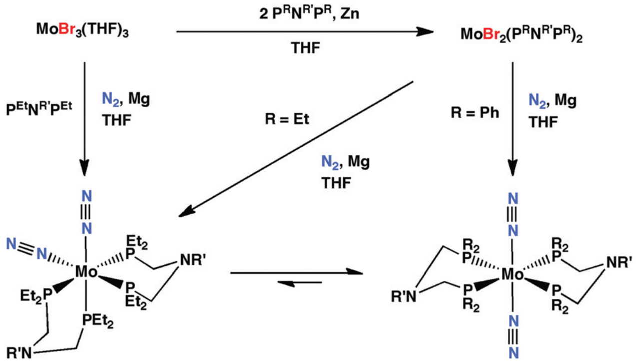

Scheme 1

Synthesis and characterization of Mo$(N_2)_2$(PNP)$_2$ complexes

To prepare the molybdenum bis(dinitrogen) complexes using the direct reduction route, $MoBr_3(THF)_3$ is stirred with magnesium powder in THF (Scheme 1) in the presence of two equivalents of PNP ligand. Contrasting isomeric products are observed depending on the identity of the substituents on phosphorus. Reactions monitored by $^{31}P\{^1H\}$ NMR and IR spectroscopy indicate that when $P^{Et}N^{Bn}P^{Et}$ ligand is used, the product *cis*-[Mo$(N_2)_2(P^{Et}N^{Bn}P^{Et})_2$] (*cis*-**5**) is formed after 2.5 h with only a minor amount of the *trans* isomer. The *cis* isomer exhibits pseudo triplets of an AA′BB′ spin system in the $^{31}P\{^1H\}$ NMR spectrum at 15.9 and 12.5 ppm and has ν_{NN} stretching bands at 1945 and 2006 in the IR. Similar results are observed with $P^{Et}N^{Me}P^{Et}$ to generate *cis*-[Mo$(N_2)_2(P^{Et}N^{Me}P^{Et})_2$] (*cis*-**6**) (see Table 2 for spectral parameters). The *cis* isomers can be isolated by concentration and cooling to −35 °C overnight, but are found to decompose over a period of 10 days in the solid state at room temperature. Upon stirring in THF for 3 days, the *cis* products are >85% converted to the *trans* isomers. *Trans*-[Mo$(N_2)_2(P^{Et}N^{Bn}P^{Et})_2$] (*trans*-**5**) and *trans*-[Mo$(N_2)_2(P^{Et}N^{Me}P^{Et})_2$] (*trans*-**6**) isolated as diamagnetic yellow solids in 64–71% yield. The $^{31}P\{^1H\}$ NMR spectrum exhibits singlet resonances at 12.4 and 12.0 ppm, respectively, as expected for a structure containing four equivalent phosphorus atoms, while the IR spectrum contains an intense ν_{NN} band at 1937 cm^{-1} for both compounds.

In contrast to the direct reduction synthesis described above, when $P^{Ph}N^{Me}P^{Ph}$ and $P^{Ph}N^{Bn}P^{Ph}$ ligands are used, better yields are obtained through a stepwise approach. The synthons **3** and **4** are reduced with Mg powder in THF, affording *trans*-[Mo$(N_2)_2(P^{Ph}N^{Me}P^{Ph})_2$] (**7-Mo**) and *trans*-[Mo$(N_2)_2(P^{Ph}N^{Bn}P^{Ph})_2$] (**8**) as yellow solids in 15–40% yield. Using this synthetic route, the *cis* isomers are not observed by $^{31}P\{^1H\}$ NMR, rather, **3** and **4** are reduced directly to the *trans* bis(dinitrogen) complexes. **7-Mo** and **8** exhibit singlets in the $^{31}P\{^1H\}$ NMR spectrum at 25.3 and 27.9 ppm and ν_{NN} bands at 1955 and 1954 cm^{-1} in the IR, respectively.

The phenylphosphine-substituted complexes exhibit ν_{NN} bands at a higher frequency than the ethyl-substituted compounds resulting from greater electron-donating ability of ethyl groups on phosphorus. This increase in phosphine electron density results in a more electron-rich metal center that can better donate electron density into N_2 π^* orbitals, weakening the N≡N bond resulting in elongation (*i.e.*, more activation).

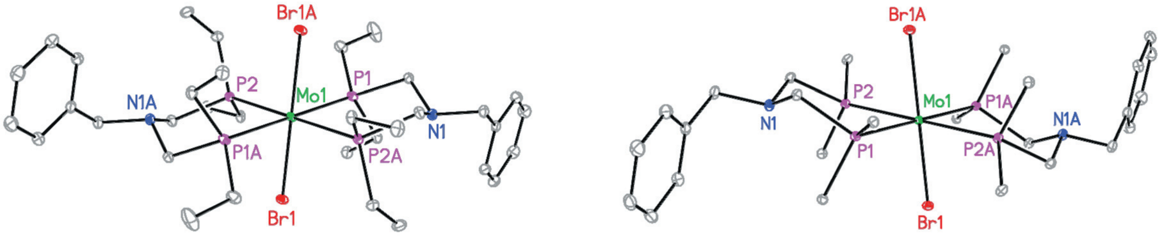

(a) *trans*-[$MoBr_2(P^{Et}N^{Bn}P^{Et})_2$] (**1**) (b) *trans*-[$MoBr_2(P^{Ph}N^{Bn}P^{Ph})_2$] (**4**)

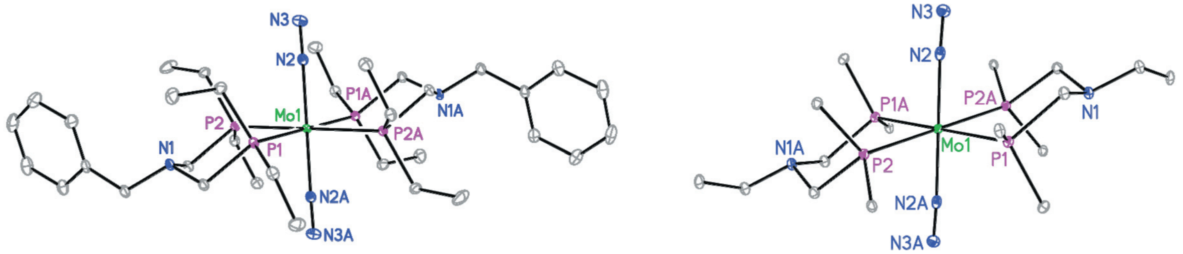

(c) *trans*-[$Mo(N_2)_2(P^{Et}N^{Bn}P^{Et})_2$] (*trans*-**5**) (d) *trans*-[$Mo(N_2)_2(P^{Ph}N^{Bn}P^{Ph})_2$] (**8**)

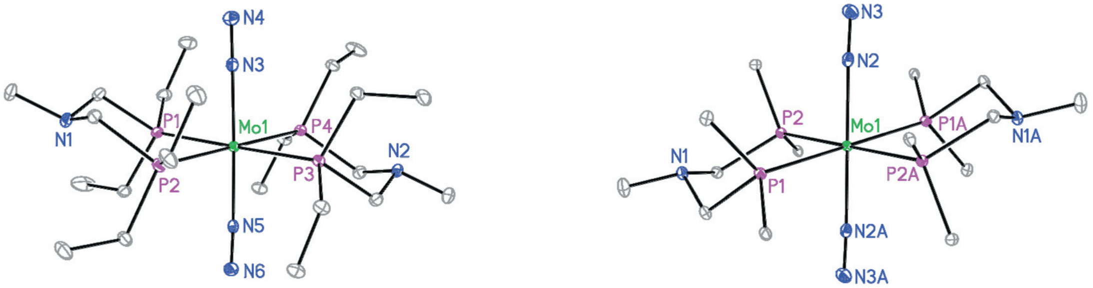

(e) *trans*-[$Mo(N_2)_2(P^{Et}N^{Me}P^{Et})_2$] (*trans*-**6**) (f) *trans*-[$Mo(N_2)_2(P^{Ph}N^{Me}P^{Ph})_2$] (**7-Mo**)

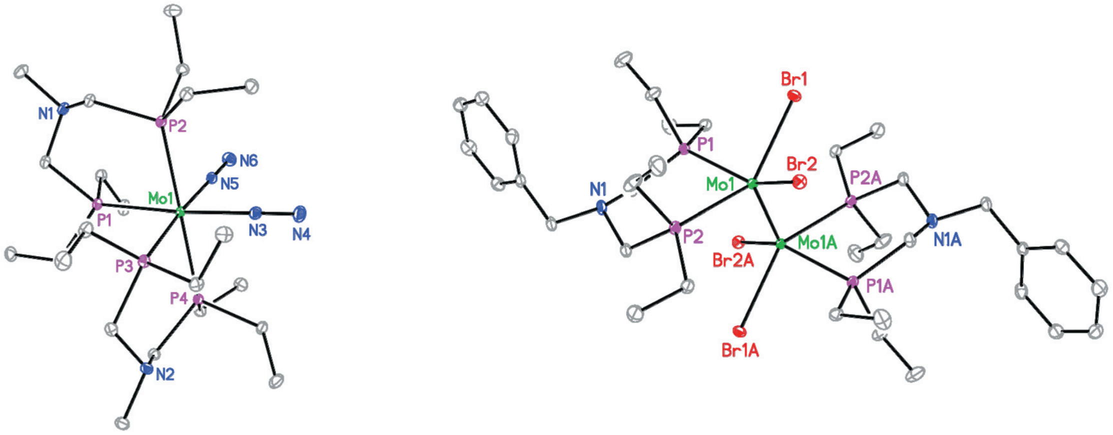

(g) *cis*-[$Mo(N_2)_2(P^{Et}N^{Me}P^{Et})_2$] (*cis*-**6**) (h) [$MoBr_2[(P^{Et}N^{Bn}P^{Et})]_2$]

Fig. 1 Molecular structures of **1** (a), **4** (b), *trans*-**5** (c), **8** (d), *trans*-**6** (e), **7-Mo** (f), *cis*-**6** (g), and $MoBr_2[(P^{Et}N^{Bn}P^{Et})]_2$ (h) with partial atom numbering. Thermal ellipsoids are drawn at 30% probability. The hydrogen atoms are omitted for clarity, and all carbons on phenyl rings except *ipso* carbons omitted in structures (b), (d) and (f).

Table 2 summarizes the IR and $^{31}P\{^1H\}$ NMR data for *cis*- and *trans*-isomers of $Mo(N_2)_2(PNP)_2$ complexes **5**–**8**.

Structural studies of molybdenum complexes

X-ray diffraction studies were carried out on crystals of dibromide complexes **1** and **4** and dinitrogen complexes, *trans*-**5**, *cis*-**6**, *trans*-**6**, **7-Mo** and **8**. The molecular structures are shown in Fig. 1 and selected metric parameters are listed in Table 1. Crystals of **1**, **4** and **7-Mo** were grown by slow evaporation of THF solution, *cis*-**6** was grown in pentane at −35 °C, while *trans*-**5** and *trans*-**6** were grown by slow evaporation of Et_2O. **8** was grown by diffusion of ether into a THF solution. General structural features of these octahedral *trans*-[$MoBr_2(PNP)_2$] and *trans*-[$Mo(N_2)_2(PNP)_2$] complexes include PNP ligand bite angles between 82 and 86°. The six-membered chelate rings of the coordinated PNP ligand are in the chair conformation and the pendant amines positioned on opposite sides of the molecule

Table 1 Selected bond lengths (Å) and angles (°) of molybdenum bis (dinitrogen) and dibromide complexes

trans-[$MoBr_2(P^{Et}N^{Bn}P^{Et})_2$] (**1**)			
Mo(1)–P(1)	2.5000(3)	P(1)–Mo(1)–P(2)	93.513(9)
Mo(1)–P(2)	2.4981(3)	P(2)–Mo(1)–P(1A)	86.487(9)
Mo(1)–Br(1)	2.57773(12)	P(1)–Mo(1)–P(1A)	180.0
		Br(1)–Mo(1)–Br(1A)	180.0
		P(2)–Mo(1)–Br(1)	86.189(7)
		P(1)–Mo(1)–Br(1)	94.805(7)
trans-[$MoBr_2(P^{Ph}N^{Bn}P^{Ph})_2$] (**4**)			
Mo(1)–P(1)	2.5566(3)	P(1)–Mo(1)–P(2)	84.528(10)
Mo(1)–P(2)	2.5164(3)	P(2)–Mo(1)–P(1A)	95.471(10)
Mo(1)–Br(1)	2.58297(12)	P(2)–Mo(1)–P(2A)	180.0
		P(2)–Mo(1)–Br(1)	93.471(8)
		P(1)–Mo(1)–Br(1)	100.520(7)
trans-[$Mo(N_2)_2(P^{Et}N^{Bn}P^{Et})_2$] (*trans*-**5**)			
Mo(1)–P(1)	2.4474(3)	P(1)–Mo(1)–P(2)	82.744(11)
Mo(1)–P(2)	2.4585(3)	P(2)–Mo(1)–P(1A)	97.255(11)
Mo(1)–N(2)	2.0163(10)	P(2)–Mo(1)–P(2A)	180.0
		N(2)–Mo(1)–N(2A)	180.0
N(2)–N(3)	1.1178(14)	N(3)–N(2)–Mo(1)	178.71(10)
		N(2)–Mo(1)–P(2)	90.21(3)
		N(2)–Mo(1)–P(1)	89.74(3)
trans-[$Mo(N_2)_2(P^{Ph}N^{Bn}P^{Ph})_2$] (**8**)			
Mo(1)–P(1)	2.4549(6)	P(1)–Mo(1)–P(2)	95.153(17)
Mo(1)–P(2)	2.4798(6)	P(2)–Mo(1)–P(1A)	84.847(17)
Mo(1)–N(2)	2.0263(17)	P(2)–Mo(1)–P(2A)	180.0
		N(2)–Mo(1)–N(2A)	180.0
N(2)–N(3)	1.116(2)	N(3)–N(2)–Mo(1)	176.91(15)
		N(2)–Mo(1)–P(2)	96.37(5)
		N(2)–Mo(1)–P(1)	86.28(5)
trans-[$Mo(N_2)_2(P^{Et}N^{Me}P^{Et})_2$] (*trans*-**6**)			
Mo(1)–P(1)	2.4470(7)	P(1)–Mo(1)–P(2)	82.83(2)
Mo(1)–P(2)	2.4469(6)	P(3)–Mo(1)–P(4)	81.95(2)
Mo(1)–P(3)	2.4406(7)	P(1)–Mo(1)–P(3)	178.800(13)
Mo(1)–P(4)	2.4491(6)	P(2)–Mo(1)–P(4)	179.731(14)
Mo(1)–N(3)	2.0220(14)	N(3)–Mo(1)–N(5)	178.48(5)
Mo(1)–N(5)	2.0215(13)	N(4)–N(3)–Mo(1)	179.56(12)
		N(6)–N(5)–Mo(1)	177.88(11)
N(3)–N(4)	1.1166(18)	N(3)–Mo(1)–P(2)	89.52(4)
N(5)–N(6)	1.1140(17)	N(3)–Mo(1)–P(1)	89.12(4)
trans-[$Mo(N_2)_2(P^{Ph}N^{Me}P^{Ph})_2$] (**7-Mo**)			
Mo(1)–P(1)	2.4758(5)	P(1)–Mo(1)–P(2)	85.924(18)
Mo(1)–P(2)	2.4493(5)	P(2)–Mo(1)–P(1A)	94.075(18)
Mo(1)–N(2)	2.0338(19)	P(2)–Mo(1)–P(2A)	180.0
		N(2)–Mo(1)–N(2A)	180.0
N(2)–N(3)	1.095(2)	N(3)–N(2)–Mo(1)	177.07(17)
		N(2)–Mo(1)–P(2)	90.42(5)
		N(2)–Mo(1)–P(1)	98.63(5)
cis-[$Mo(N_2)_2(P^{Et}N^{Me}P^{Et})_2$] (*cis*-**6**)			
Mo(1)–P(1)	2.4650(4)	P(1)–Mo(1)–P(2)	85.378(12)
Mo(1)–P(2)	2.4617(4)	P(3)–Mo(1)–P(4)	82.780(13)
Mo(1)–P(3)	2.4635(4)	P(1)–Mo(1)–P(3)	95.501(13)
Mo(1)–P(4)	2.4500(4)	P(2)–Mo(1)–P(4)	177.296(14)
Mo(1)–N(3)	2.0287(12)	N(3)–Mo(1)–N(5)	85.79(5)
Mo(1)–N(5)	2.0143(13)	N(4)–N(3)–Mo(1)	175.93(13)
		N(6)–N(5)–Mo(1)	177.54(12)
N(3)–N(4)	1.1226(17)	N(3)–Mo(1)–P(2)	92.86(3)
N(5)–N(6)	1.1216(18)	N(3)–Mo(1)–P(1)	173.82(4)

with amine substituents in the equatorial positions. For *cis*-**6** the pendant amines are positioned so the lone pair electrons are facing the adjacent N_2 ligand. The Mo–P bond lengths for **1** (Fig. 1a), are 2.5000(3) and 2.4981(3) Å, while those for **4** (Fig. 1b) are slightly longer at 2.5566(3) and 2.5164(3) Å. In the structure of *trans*-**5** (Fig. 1c), the Mo–P bond lengths are shorter than those for the dibromide complexes at 2.4585(3), 2.4474(3) Å. The average Mo–P bond length of 2.4460(3) Å was determined for *trans*-**6**, which is slightly shorter than the average Mo–P bond length in *cis*-**6** (Fig. 1g) at 2.4600(4) Å. In **7-Mo** (Fig. 1f) the Mo–P bonds are 2.4493(5) and 2.4758(5) Å, while in **8** (Fig. 1d) they are 2.4549(6) and 2.4798(6) Å. Upon binding to Mo, the dinitrogen bond length becomes longer compared to free N_2 at 1.0975 Å.[4a,20] With an electron-rich metal center, *trans*-**5** and *trans*-**6** the $N\equiv N$ bond distances are 1.118(1) and (1.117(2), 1.114(2)) Å, respectively, indicating slight activation of N_2. The $N\equiv N$ bond length is slightly longer for *cis*-**6** (compared to *trans*-**6**) at 1.123(2) and 1.121(2) Å, due to the N_2 ligands position *trans* to a phosphine donor.[21] Elongation of the $N\equiv N$ bond is expected for **7-Mo** and **8**, given the similar red shifted ν_{NN} band in the IR, however, while the $N\equiv N$ bond length of **8** is in the expected range at 1.116(2) Å, the $N\equiv N$ bond length of 1.095(2) Å for **7-Mo** is not elongated compared to free N_2.

Synthesis and characterization of tungsten complexes *trans*-[$W(N_2)_2$(dppe)(PNP)] and *trans*-[$W(N_2)_2(PNP)_2$]

The synthesis of tungsten–phosphine bis(dinitrogen) complexes is well established, and many complexes have been prepared through reduction of WCl_6, WCl_4(dppe) or $WCl_4(PPh_3)_2$ by Mg or Na–Hg.[22,14a] The latter two are utilized here and are synthesized by zinc reduction of WCl_6 with PPh_3 to afford $WCl_4(PPh_3)_2$ (eqn (1)) followed by phosphine ligand exchange at W(IV) to afford WCl_4(dppe) (eqn (2)). *Trans*-[$W(N_2)_2$(dppe)(PNP)] mixed complexes are prepared by reduction of WCl_4(dppe) with one equivalent of the desired PNP ligand and excess Mg powder in THF under an atmosphere of N_2 (eqn (3)).

$$WCl_6 \quad + \quad (xs)\ PPh_3 \xrightarrow[CH_2Cl_2]{Zn} WCl_4(PPh_3)_2 \qquad (1)$$

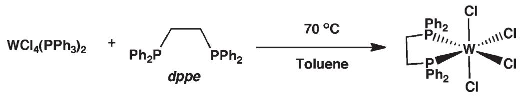

(2)

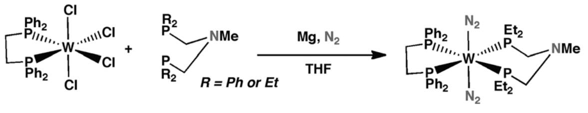

(3)

The complexes *trans*-[$W(N_2)_2$(dppe)($P^{Et}N^{Me}P^{Et}$)] (**9**) and *trans*-[$W(N_2)_2$(dppe)($P^{Ph}N^{Me}P^{Ph}$)] (**10**), were obtained using this procedure, the latter of which has been previously reported by Tuczek and coworkers.[11] The $^{31}P\{^1H\}$ NMR spectrum for **9** exhibits two AA′XX′ multiplet resonances at 45.6 and −13.2 ppm with ^{183}W satellites (J_{P-W} = 319 and 302 Hz, respectively). The IR spectrum for **9** contains a strong asymmetric ν_{NN} band at 1921 cm^{-1} and a weak symmetric ν_{NN} band at 1990 cm^{-1}, similar to **10**. Despite the electron-donating phosphine substituents, the ν_{NN} band for **9** is at 11 cm^{-1} higher frequency than **10** (Table 2). The isotopically-labelled complex *trans*-[$W(^{15}N_2)_2$(dppe)($P^{Et}N^{Me}P^{Et}$)] (**9-^{15}N$_2$**) was prepared using $^{15}N_2$ gas, resulting in an asymmetric ν_{NN} band at 1859 cm^{-1}, a 62 cm^{-1} shift *versus* the unlabelled complex.[23]

Attempts to incorporate PNP ligand variants $P^{Et}N^{Bn}P^{Et}$, $P^{Ph}N^{Ph}P^{Ph}$, $P^{Cy}N^{Me}P^{Cy}$ and $P^{Cy}N^{Bn}P^{Cy}$ into *trans*-[$W(N_2)_2$(dppe)(PNP)] proved to be challenging. Using $P^{Et}N^{Bn}P^{Et}$, *trans*-[$W(N_2)_2$(dppe)($P^{Et}N^{Bn}P^{Et}$)] (**11**) was formed based on $^{31}P\{^1H\}$ NMR (45.5 and −14.0 ppm with J_{P-W} = 319 and 303 Hz

Table 2 Summary of $^{31}P\{^1H\}$, IR, crystallographic, and electrochemical data for W and Mo bis(dinitrogen) complexes

Compound	^{31}P NMR[a]	ν_{NN}[b] (asym)	ν_{NN}[b] (sym)	M–N[e]	N–N[e]	$E_{1/2}$[h]
trans-$[Mo(N_2)_2(P^{Et}N^{Bn}P^{Et})_2]$ (*trans*-**5**)	12.4	1937	2006	2.016(1)	1.118(1)	−1.06
cis-$[Mo(N_2)_2(P^{Et}N^{Bn}P^{Et})_2]$ (*cis*-**5**)	15.9; 12.5	1945	2006	—	—	—
trans-$[Mo(N_2)_2(P^{Et}N^{Me}P^{Et})_2]$ (*trans*-**6**)	12.0	1937	—	2.022(1)	1.114(2) 1.117(2)	−1.07
cis-$[Mo(N_2)_2(P^{Et}N^{Me}P^{Et})_2]$ (*cis*-**6**)	15.2; 12.8	1941	2007	2.014(1) 2.029(1)	1.123(2) 1.122(2)	—
trans-$[Mo(N_2)_2(P^{Ph}N^{Me}P^{Ph})_2]$ (**7-Mo**)	25.3	1955	—	2.034(2)	1.095(2)	−0.82
trans-$[Mo(N_2)_2(P^{Ph}N^{Bn}P^{Ph})_2]$ (**8**)	27.9	1954	2020	2.026(2)	1.116(2)	−0.81
trans-$[W(N_2)_2(dppe)(P^{Et}N^{Me}P^{Et})]$ (**9**)	45.6; −13.2	1921	1990	2.020(2) 2.010(2)	1.129(2) 1.128(2)	−0.96
trans-$[W(N_2)_2(dppe)(P^{Ph}N^{Me}P^{Ph})]$ (**10**)	41.4; 4.3[c]	1910[c]	2013[c]	2.033(1) 2.001(1)	1.130(2) 1.120(2)	−0.83
trans-$[W(N_2)_2(dppe)(P^{Et}N^{Bn}P^{Et})]$ (**11**)	45.5; −14.0	1922	1990	—	—	—
trans-$[W(N_2)_2(P^{Ph}N^{Me}P^{Ph})_2]$ (**7-W**)	−3.1	1925	2027	2.021(2)	1.103(3)	−0.80
trans-$[W(N_2)_2(P^{Et}N^{Me}P^{Et})_2]$ (*trans*-**12**)	−15.2	1942[d]	—	—	—	—
cis-$[W(N_2)_2(P^{Et}N^{Me}P^{Et})_2]$ (*cis*-**12**)	−12.1; −13.7	1916	1981	—	—	—
trans-$[W(N_2)_2(dppe)(dppp)]$ (**13**)	44.2; 1.5	1917	1995	—	—	−0.79
trans-$[W(N_2)_2(dppp)_2]$ (**14**)	−3.3	1912	—	1.996(2)	1.125(3)	—
trans-$[W(N_2)_2(PPh_2Me)_4]$	−9.4	1900	1973	1.991(1)[f] 2.001(1)	1.134(2)[f] 1.132(2)	—
trans-$[W(N_2)_2(dppe)_2]$	46.5	1943	2008	1.996(11) 1.985(10)[g]	1.126(15) 1.141(16)[g]	−0.82

[a] $^{31}P\{^1H\}$ NMR (ppm) spectra were collected in THF and referenced against H_3PO_4. [b] IR (cm^{-1}) spectra were collected as KBr pellets. [c] Ref. 11. [e] In hexanes. [e] Bond lengths reported in Å. [f] See ESI† for X-ray structure. [g] Ref. 25. [h] Cyclic voltammetry performed in THF–$^nBu_4NB(C_6F_5)_4$ (0.2 M) at 0.1 V s^{-1}. The $E_{1/2}$ values are for reversible $M^{I/0}$ couples.

^{183}W satellites, respectively) and IR (ν_{NN} at 1922(s) and 1990 (w) cm^{-1}) data, however it was not successfully isolated in pure form. Using $P^{Ph}N^{Ph}P^{Ph}$, a paramagnetic product was obtained. The $^{31}P\{^1H\}$ NMR spectrum shows the liberation of PPh_3 and consumption of free $P^{Ph}N^{Ph}P^{Ph}$, indicating ligand exchange, but no ν_{NN} bands were observed in the IR spectrum. The use of $P^{Cy}N^{Bn}P^{Cy}$ and $P^{Cy}N^{Me}P^{Cy}$ resulted in unidentified products as determined by $^{31}P\{^1H)$ NMR, and no ν_{NN} bands were observed in the IR spectrum.

To prepare tungsten bis(dinitrogen) complexes containing two PNP ligands (*i.e.*, *trans*-$[W(N_2)_2(PNP)_2]$), two equivalents of $P^RN^{Me}P^R$ ligand (R = Ph, Et, Cy) were mixed with $WCl_4(PPh_3)_2$ in THF with excess Mg powder and stirred under N_2 for a minimum of 18 h. An orange solid was collected using $P^{Ph}N^{Me}P^{Ph}$ and $P^{Cy}N^{Me}P^{Cy24}$ and a yellow oil was obtained for $P^{Et}N^{Me}P^{Et}$. *Trans*-$[W(N_2)_2(P^{Ph}N^{Me}P^{Ph})_2]$ (**7-W**) was recrystallized from THF or toluene and obtained in a 9% crystalline yield (eqn (4a)).

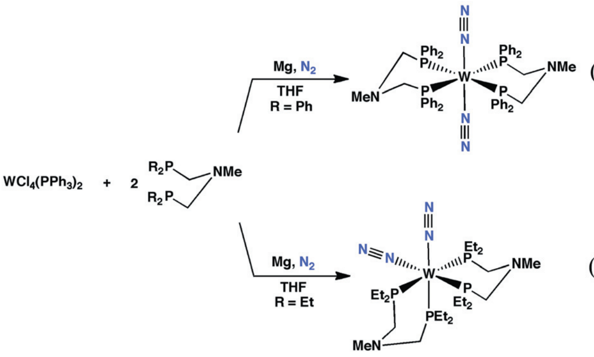

(4a)

(4b)

(4)

The $^{31}P\{^1H\}$ NMR spectrum shows a singlet resonance at −3.1 ppm with $J_{P–W}$ = 308 Hz ^{183}W satellites while the IR spectrum contains a strong asymmetric ν_{NN} band at 1925 cm^{-1} and a weak symmetric ν_{NN} band at 2027 cm^{-1}. The isotopically-labelled *trans*-$[W(^{15}N_2)_2(P^{Ph}N^{Me}P^{Ph})_2]$ (**7-W^{15}N$_2$**) exhibits a strong ν_{NN} band at 1867 and a weak band at 1959 cm^{-1} (Fig. 2). After degassing and placing the sample under Ar, a ^{15}N NMR spectrum of **7-W^{15}N$_2$** was collected at 25 °C in THF. Two strong resonances at −51 (doublet, $J_{N–N}$ = 5.3 Hz) and −62 (multiplet with $J_{N–W}$ = 52 Hz ^{183}W satellites) ppm were observed and assigned to the distal and proximal tungsten-bound dinitrogen atoms, respectively (referenced to $CH_3{}^{15}NO_2$, δ = 0). A small amount of free $^{15}N_2$ gas is observed at −73 ppm indicating liberation of tungsten-bound $^{15}N_2$ in THF (see ESI† for spectrum).[26]

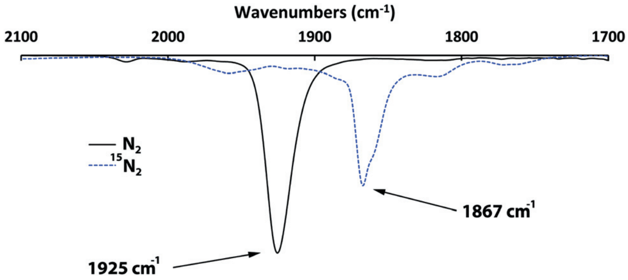

Fig. 2 Infrared spectra (KBr) of $^{15}N_2$ labelled (dotted) and unlabelled (black) *trans*-$[W(N_2)_2(P^{Ph}N^{Me}P^{Ph})_2]$ (**7-W**). The asymmetric tungsten N_2 stretch is shifted by 58 cm^{-1} as a result of the isotopic labelling.

In contrast, when the reduction is performed using $P^{Et}N^{Me}P^{Et}$ ligand, *cis*-$[W(N_2)_2(P^{Et}N^{Me}P^{Et})_2]$ (*cis*-**12**, eqn (4b)) was obtained based on $^{31}P\{^1H\}$ NMR, virtual triplets of an AA′BB′ pattern at −12.1 and −13.7 ppm with $J_{P–W}$ = 296 and 304 Hz ^{183}W satellites, respectively, as a yellow oil with <5% *trans*-$[W(N_2)_2(P^{Et}N^{Me}P^{Et})_2]$ (*trans*-**12**). *Trans*-**6** exhibits a singlet at −15.2 ppm with $J_{P–W}$ = 303 Hz ^{183}W satellites. However, due to the high solubility of these products in organic solvents, *cis*-**12** and *trans*-**12** compounds could not be completely isolated from the free ligand and were not obtained pure. Isomerization occurs slowly, over a period of 4 months in pentane at −35 °C, after this time *trans*-**12** had increased to ~25% by $^{31}P\{^1H\}$ NMR.

trans-[W(N_2)$_2$(dppe)(dppp)] and *trans*-[W(N_2)$_2$(dppp)$_2$]

As a comparison for the structural and spectroscopic analysis of the mixed *trans*-[W(N_2)$_2$(dppe)(PNP)] complexes **9** and **10**, the analogous tungsten bis(dinitrogen) complex, *trans*-[W(N_2)$_2$(dppe)(dppp)] (**13**) (dppp = 1,3-bis(diphenylphosphino)propane) without a pendant amine was prepared. WCl_4(dppe) was stirred in THF with Mg powder and 1 equiv. dppp, affording **13** as a red–orange microcrystalline solid in 5% yield. The $^{31}P\{^1H\}$ NMR spectrum contains AA′XX′ resonances at 44.2 and 1.5 ppm ($J_{P–W}$ = 311 and 314 Hz ^{183}W satellites, respectively) corresponding to the dppe and dppp ligands, respectively. The product also contained ~15% *trans*-[W(N_2)$_2$(dppe)$_2$] (a singlet at 46.5 ppm in THF in the $^{31}P\{^1H\}$ NMR spectrum). The separation of the two compounds has not been achieved. The IR spectrum of **13** contains an asymmetric ν_{NN} band at 1917 cm^{-1}, which is slightly higher in energy than the asymmetric ν_{NN} band for **10** at 1910 cm^{-1}.[11] Efforts to prepare *trans*-[W(N_2)$_2$(dppp)$_2$] (**14**) by the procedure used for *trans*-[W(N_2)$_2$(PNP)$_2$] complexes resulted in formation of the target complex only as a minor product, exhibiting a singlet at −3.3 ppm in the $^{31}P\{^1H\}$ NMR with $J_{P–W}$ = 307 Hz ^{183}W satellites, among multiple unidentified tungsten–phosphine products by $^{31}P\{^1H\}$ NMR resonances with ^{183}W satellites.[27] The IR spectrum contained a single asymmetric ν_{NN} band at 1912 cm^{-1}. Because **14** was a minor product in this complex mixture, only a few small crystals could be isolated, but a full spectroscopic analysis was performed. The difficulty synthesizing **14** is surprising considering the prevalence of *trans*-[W(N_2)$_2$(dppe)$_2$] in the literature[6d,28] and may be due to the formation of a less favorable six-membered ring upon coordination of PNP ligand to the metal in the resulting complex.

Structural studies

X-ray crystallographic studies were performed for the *trans*-[W(N_2)$_2$(dppe)(PNP)] complexes **9** and **10** as well as **7-W** and the non-pendant amine containing complex **14**. Crystals were grown in THF at −35 °C or by slow evaporation at room temperature. The molecular structures are shown in Fig. 3 and selected bond lengths and angles are listed in Table 3. Each complex exhibits octahedral geometry with the bidentate PNP, dppe and/or dppp ligands in the equatorial plane and the dinitrogen ligands in the axial positions. For the mixed ligand complexes **9** and **10**, the PNP or dppp ligand forms a six-membered ring upon coordination to the metal center; all of these six-membered rings adopt a chair conformation. For **7-W** and **14** the six-membered ring also resides in the chair conformation with the pendant amines or central methylene group from one ligand pointing in the opposite direction as the other pendant amine or methylene group for the second ligand. The bite angles for the PNP/dppp and dppe ligands are in the range 83–85° and 79–80°, respectively. The N–W–N bond angles of the dinitrogen ligands are 180° for the bis(PNP) and bis(dppp) complexes **7-W**, *trans*-**12**, and **14**, due to crystallographic symmetry. The N–W–N bond angles for the heteroleptic complexes **9** and **10** deviate slightly from linearity at 173.83(7)° and 173.35(5)°. The W–P bond lengths fall between 2.43–2.48 Å.

As observed in the Mo bis(dinitrogen) complexes, coordination of dinitrogen to tungsten results in weak activation of dinitrogen indicated by lengthening of the N≡N bond compared to free N_2 (1.0975 Å).[4a,20] The degree of N_2 activation, determined by IR and X-ray crystallography, typically follows the trend where complexes containing electron-donating substituents exhibit ν_{NN} bands that occur at lower energy and exhibit slightly longer N–N bond distances.[4a] The Mo- and W-N_2 PNP complexes reported here follow these trends with the exception of the mixed phosphine complexes **9** and **10**, where the N≡N bond lengths are nearly identical and the asymmetric ν_{NN} band for **10** (1910 cm^{-1}) is 11 cm^{-1} lower in energy than **9** (1921 cm^{-1}), despite the electron withdrawing phenyl substituents on PNP phosphorus atoms. We suggest that the reason the less electron-rich metal center in **10** exhibits the more activated N–N bond could be due to the greater steric requirement of the phenyl groups of the PNP ligand *versus* ethyl groups. The bulky phenyl groups cause the W–N–N bond angle to deviate from linearity, as a result, more effective orbital overlap leads to increased back-donation from the metal to π* orbitals of N_2, weakening the N–N bond.[21b,29] A similar observation is observed for complex **14** and **7-W** where **14** exhibits a longer N≡N bond (1.125 Å) and is more red shifted ν_{NN} band (1912 cm^{-1}) than **7-W** (1.103 Å and 1925 cm^{-1}) despite identical ligand ring size and phenyl substituents on phosphorus atoms. The pendant methylamine group in the ligand backbone of **7-W** is not expected to have a significant electronic effect. As the W–N–N bond angles deviate from linearity to a slightly greater extent in compound **14** (175.6(2)°) *versus* **7-W** (177.9(2)°), this deviation may again contribute to the weakening of the N–N bond as observed in the IR. A comparison of M–N_2 and N–N bond distances between analogous complexes **7-Mo** and **7-W** shows that dinitrogen is more strongly activated in the tungsten complex. The ν_{NN} bands are consistent with these crystallographic observations, with the **7-W** complex exhibiting a 30 cm^{-1} lower frequency (*i.e.*, more activated N_2) than **7-Mo**. The greater N_2 activation by **7-W** can also be explained by the more electron releasing nature of tungsten compared to molybdenum.[21b,30]

An X-ray crystallographic study performed on crystals grown from the reaction intended to produce the mixture of *cis*-**12** and *trans*-**12** consisted of a mixture of *trans*-**12** and *trans*-[WCl_2($P^{Et}N^{Me}P^{Et}$)$_2$], Fig. 3f. From the X-ray data, the occupancy of N_2 to Cl was modelled at a 25 : 75 ratio.[31] The N–N bond distance was determined to be 1.16(2) Å; however, because of the N_2 and Cl ligand disorder, the accuracy of this bond distance is less reliable (see ESI† for crystallographic metrics). The complex *cis*-[WCl_2($P^{Et}N^{Me}P^{Et}$)$_2$], Fig. 3e, was also obtained from this reaction. The six-coordinate *cis*-dichloride complex exhibits a highly distorted octahedral geometry. To our knowledge, the only other structural report of a tungsten *cis*-dichloride complex is *cis*-[WCl_2(depe)$_2$] which exhibits a nearly identical distorted octahedral structure.[32]

Electrochemical studies

Cyclic voltammetry experiments of the molybdenum and tungsten bis(dinitrogen) complexes were performed in THF using 0.2 M [$^nBu_4N$][$B(C_6F_5)_4$] as the supporting electrolyte. All potentials are reported *versus* the ferrocene–ferrocenium couple at 0 V. Table 4 summarizes the electrochemical data for all complexes

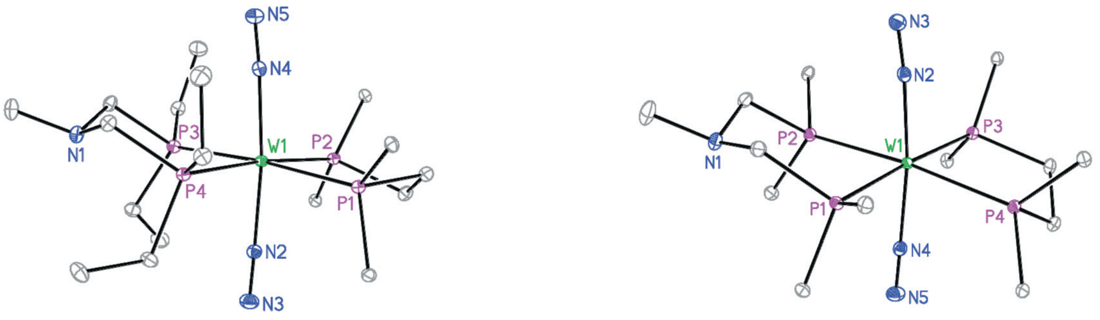

(a) *trans*-[W(N$_2$)$_2$(dppe)(P^{Et}N^{Me}P^{Et})] (**9**)

(b) *trans*-[W(N$_2$)$_2$(dppe)(P^{Ph}N^{Me}P^{Ph})] (**10**)

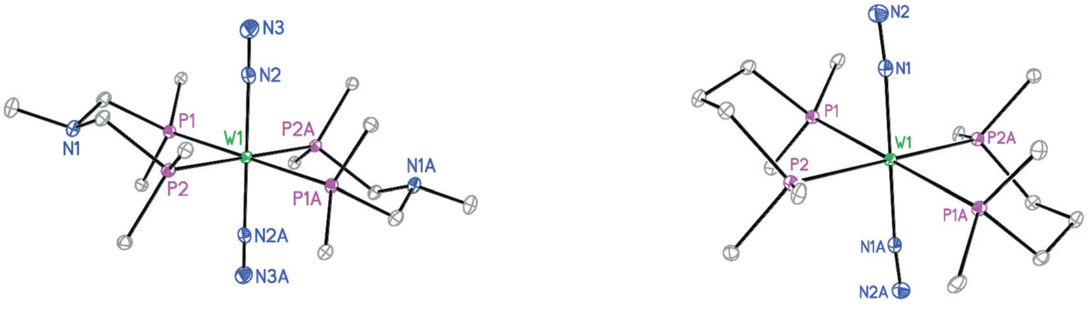

(c) *trans*-[W(N$_2$)$_2$(P^{Ph}N^{Me}P^{Ph})$_2$] (**7-W**)

(d) *trans*-[W(N$_2$)$_2$(dppp)$_2$] (**14**)

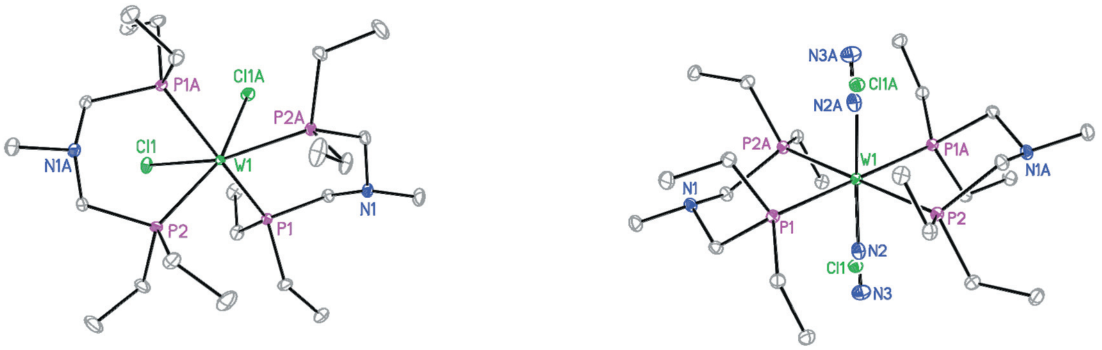

(e) *cis*-[WCl$_2$(P^{Et}N^{Me}P^{Et})$_2$]

(f) *trans*-[W(N$_2$)$_2$(P^{Et}N^{Me}P^{Et})$_2$] (*trans*-**12**)

Fig. 3 Molecular structures of **9** (a), **10** (b), **7-W** (c), **14** (d), *cis*-[WCl$_2$(P^{Et}N^{Me}P^{Et})$_2$] (e), and *trans*-**12**. Thermal ellipsoids are drawn at 30% probability. Only *ipso* carbons on the dppe, dppp, and P^{Ph}N^{Me}P^{Ph} phosphine phenyls are shown. The hydrogen atoms are omitted for clarity. The structure of *trans*-**12** consists of *trans*-[WCl$_2$(P^{Et}N^{Me}P^{Et})$_2$] and *trans*-[W(N$_2$)$_2$(P^{Et}N^{Me}P^{Et})$_2$] with the occupancy of N$_2$ to Cl modelled at a 25 : 75 ratio.

examined in this study (see the ESI† for all cyclic voltammograms). The oxidation potentials for the Mo and W M$^{I/0}$ and M$^{II/I}$ waves are related to the electron-donating ability of the substituents on phosphorus. Thus, the complexes that contain electron-donating ethyl groups exhibit M$^{I/0}$ waves at more negative potentials (−0.30 V) compared to those with phenyl groups on phosphorus. The M$^{I/0}$ couples fall between the range of −0.80 to −1.07 V, and the peak potential for the irreversible M$^{II/I}$ couple is between 0.01 to 0.18 V. No reduction of the complexes was observed, even at potentials as low as −2.0 V.[33]

The cyclic voltammogram of **9**, shown in Fig. 4, consists of a reversible W$^{I/0}$ couple, $E_{1/2}$ = (−0.96 V, and an irreversible W$^{II/I}$ wave with a peak potential, E_{pa} = 0.04 V. For all complexes containing PNP ligands in this study, an irreversible M$^{II/I}$ wave was observed, with no change in irreversibility at scan rates up to 0.5 V s^{-1}. However, with the exception of **9**, when scanning through both M$^{I/0}$ and M$^{II/I}$ couples, loss of current is observed on the return scan for the M$^{I/0}$ couple, resulting in a quasireversible M$^{I/0}$ wave. Scanning through the M$^{I/0}$ couple before reaching the M$^{II/I}$ wave, results in a M$^{I/0}$ couple that exhibits no loss of current. The loss of current for cathodic portion of the M$^{I/0}$ wave after reaching the potential of the M$^{II/I}$ wave is likely due to loss of one or both bound dinitrogen ligands upon oxidation to M^{2+} state. In contrast to the tungsten bis(dinitrogen) PNP-containing complexes, the W bis(dinitrogen) complexes without pendant amines, *e.g.* **13**, exhibit a quasireversible M$^{II/I}$ couple (Fig. 5). The electrochemical reversibility of this wave is scan rate dependant, becoming more reversible at faster scan rates, *i.e.* 0.5 V s^{-1} (see ESI† for details). Performing the cyclic voltammogram under an Ar atmosphere does not change the quasi-reversible nature of the M$^{II/I}$ couple at 0.1 V s^{-1}, suggesting that the N$_2$ ligands may not be liberated from the metal center as readily as in the pendant amine containing complexes. We postulate that pendant amine could promote N$_2$ ligand loss by interacting with the M^{2+} center. This type of interaction has been observed with a Cr complex containing ligands with pendant amines.[10]

Table 3 Selected bond lengths (Å) and angles (°) of tungsten bis(dinitrogen) complexes

trans-[W(N_2)$_2$(dppe)($P^{Et}N^{Me}P^{Et}$)] (**9**)			
W(1)–P(1)	2.4313(5)	P(1)–W(1)–P(2)	80.250(18)
W(1)–P(2)	2.4385(5)	P(3)–W(1)–P(4)	84.708(18)
W(1)–P(3)	2.4542(5)	P(1)–W(1)–P(3)	175.149(19)
W(1)–P(4)	2.4407(5)	N(2)–W(1)–N(4)	173.83(7)
W(1)–N(4)	2.0102(19)	N(3)–N(2)–W(1)	177.58(17)
W(1)–N(2)	2.020a0(18)	N(5)–N(4)–W(1)	176.31(17)
N(2)–N(3)	1.128(2)	N(2)–W(1)–P(1)	86.56(5)
N(4)–N(5)	1.129(2)	N(2)–W(1)–P(3)	88.67(5)
trans-[W(N_2)$_2$(dppe)($P^{Ph}N^{Me}P^{Ph}$)] (**10**)			
W(1)–P(1)	2.4305(4)	P(1)–W(1)–P(2)	85.307(13)
W(1)–P(2)	2.4333(4)	P(3)–W(1)–P(4)	79.444(13)
W(1)–P(3)	2.4552(4)	P(1)–W(1)–P(3)	176.757(13)
W(1)–P(4)	2.4553(4)	N(2)–W(1)–N(4)	173.35(5)
W(1)–N(4)	2.0326(13)	N(3)–N(2)–W(1)	175.05(12)
W(1)–N(2)	2.0011(13)	N(5)–N(4)–W(1)	178.42(14)
N(2)–N(3)	1.1301(18)	N(2)–W(1)–P(1)	85.15(4)
N(4)–N(5)	1.1195(19)	N(2)–W(1)–P(3)	97.07(4)
trans-[W(N_2)$_2$($P^{Ph}N^{Me}P^{Ph}$)$_2$] (**7-W**)			
W(1)–P(1)	2.4410(6)	P(1)–W(1)–P(2)	85.15(2)
W(1)–P(2)	2.4710(6)	P(1A)–W(1)–P(2A)	85.15(2)
W(1)–P(1A)	2.4410(6)	P(1)–W(1)–P(1A)	180.0
W(1)–P(2A)	2.4710(6)	N(2)–W(1)–N(2A)	180.0
W(1)–N(2)	2.021(2)	N(3)–N(2)–W(1)	177.9(2)
W(1)–N(2A)	2.021(2)		
		N(2)–W(1)–P(1)	90.22(6)
N(2)–N(3)	1.103(3)	N(2)–W(1)–P(1A)	89.78(6)
trans-[W(N_2)$_2$(dppp)$_2$] (**14**)			
W(1)–P(1)	2.4692(7)	P(1)–W(1)–P(2)	85.37(2)
W(1)–P(2)	2.4792(6)	P(1A)–W(1)–P(2A)	85.37(2)
W(1)–P(1A)	2.4691(7)	P(1)–W(1)–P(1A)	180.00(3)
W(1)–P(2A)	2.4793(6)	N(2)–W(1)–N(2A)	180.0
W(1)–N(1)	1.996(2)	N(2)–N(1)–W(1)	175.6(2)
W(1)–N(1A)	1.996(2)		
		N(1)–W(1)–P(1)	82.99(6)
N(1)–N(2)	1.125(3)	N(1)–W(1)–P(1A)	97.01(6)

Table 4 Redox couples (V *vs.* $Cp_2Fe^{+/0}$) for Mo and W PNP complexes performed in THF–$^nBu_4NB(C_6F_5)_4$ (0.2 M) at 0.1 V s^{-1}

Complexes	$M^{I/0}$ ($E_{1/2}$)	$M^{II/I}$ (E_{pa})
trans-[Mo(N_2)$_2$($P^{Et}N^{Me}P^{Et}$)$_2$] (*trans*-**6**)	−1.07	0.01
trans-[Mo(N_2)$_2$($P^{Et}N^{Bn}P^{Et}$)$_2$] (*trans*-**5**)	−1.06	0.02
trans-[Mo(N_2)$_2$($P^{Ph}N^{Me}P^{Ph}$)$_2$] (**7-Mo**)	−0.82	0.18
trans-[Mo(N_2)$_2$($P^{Ph}N^{Bn}P^{Ph}$)$_2$] (**8**)	−0.81	0.23
trans-[W(N_2)$_2$($P^{Ph}N^{Me}P^{Ph}$)$_2$] (**7-W**)	−0.80	0.07
trans-[W(N_2)$_2$(dppe)($P^{Et}N^{Me}P^{Et}$)] (**9**)	−0.96	0.04
trans-[W(N_2)$_2$(dppe)($P^{Ph}N^{Me}P^{Ph}$)] (**10**)	−0.79	0.14
trans-[W(N_2)$_2$(dppe)(dppp)] (**13**)	−0.83	0.24[a]
trans-[W(N_2)$_2$(dppe)$_2$]	−0.82	0.22[a]

[a] $E_{1/2}$ for quasireversible $M^{II/I}$ couples.

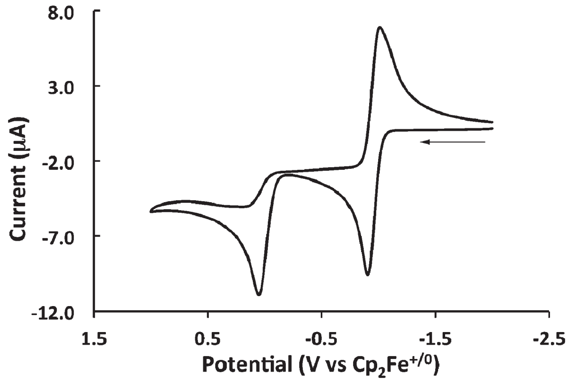

Fig. 4 Cyclic voltammogram of *trans*-[W(N_2)$_2$(dppe)($P^{Et}N^{Me}P^{Et}$)] in THF–$^nBu_4NB(C_6F_5)_4$ (0.2 M) at 0.1 V s^{-1} showing a reversible $M^{I/0}$ couple at −0.96 V and an irreversible $M^{II/I}$ couple at 0.04 V. Referenced to ferrocenium–ferrocene (0.0 V).

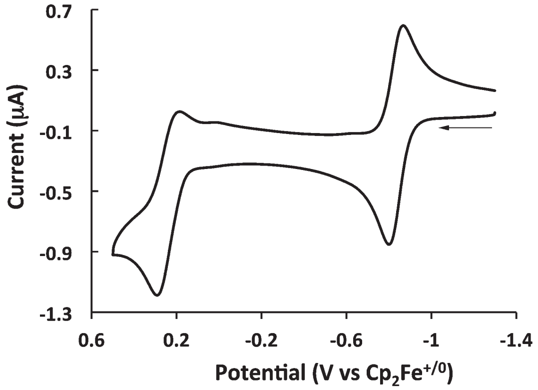

Fig. 5 Cyclic voltammogram of *trans*-[W(N_2)$_2$(dppe)(dppp)] in THF–$^nBu_4NB(C_6F_5)_4$ (0.2 M) at 0.1 V s^{-1} showing a reversible $M^{I/0}$ couple at −0.83 V and a quasireversible $M^{II/I}$ couple at 0.24 V.

Reactions of Mo and W complexes with CO

To examine the reactivity of the PNP-containing Mo and W bis(dinitrogen) complexes, reactivity studies with CO were carried out on selected complexes. In a typical experiment, a solution of the Mo or W dinitrogen complex in an NMR tube was exposed to 1 atm CO at room temperature. The treatment of a mixture of *cis*-**5** and *trans*-**5** with CO indicates the *cis* isomer reacts quickly, ejecting both equivalents of N_2, fully converting to *cis*-[Mo(CO)$_2$($P^{Et}N^{Bn}P^{Et}$)$_2$], **15**, in less than 5 min. **15** exhibits two multiplets at 15.4 and 3.1 ppm in the $^{31}P\{^1H\}$ NMR spectrum. *Trans*-**5** requires 40 h at room temperature to proceed to >92% conversion to **15**, which exhibits ν_{CO} bands at 1837 and 1768 cm^{-1}, similar to other Mo(CO)$_2$ complexes.[34] When the reaction is performed with ^{13}CO, the ν_{CO} bands shift to 1802 and 1742 cm^{-1}.

In contrast to the isomerization of *trans*-**5** to **15**, when a solution of **7-Mo** is exposed to a ^{13}CO atmosphere, the initial $^{31}P\{^1H\}$ NMR spectrum recorded after 3 h showed a ~1 : 1 mixture of **7-Mo** and *trans*-[Mo(CO)$_2$($P^{Ph}N^{Me}P^{Ph}$)$_2$] (*trans*-**16**), identified by a triplet resonance at 31.4 ppm ($J_{P–C}$ = 9.0 Hz) and a single asymmetric ν_{13CO} band in the IR at 1885 cm^{-1}. After 24 h, *cis*-[Mo(^{13}CO)$_2$($P^{Ph}N^{Me}P^{Ph}$)$_2$] (*cis*-**16**) was identified in ~2 : 1 *cis*–*trans* Mo(CO)$_2$ ratio by $^{31}P\{^1H\}$ NMR, by two multiplets at 27.5 and 12.3 ppm. The IR spectrum contains ν_{13CO} bands of nearly equal intensity at 1834 and 1772 cm^{-1}. Loss of the PNP ligand from Mo was evident after this time by the presence of free ligand in the $^{31}P\{^1H\}$ NMR spectrum.

The addition of one atmosphere of CO to **9** in THF leads to the formation of *cis*-[W(CO)$_2$(dppe)($P^{Et}N^{Me}P^{Et}$)] (**17**) over the course of 72 h. The $^{31}P\{^1H\}$ NMR spectrum indicated the disappearance of the multiplet resonances at 45.6 and −13.2 ppm corresponding to **9** and the appearance of four ddd resonances at

46.8 (dppe), 39.9 (dppe), −11.2 ($P^{Et}N^{Me}P^{Et}$), and −24.5 ($P^{Et}N^{Me}P^{Et}$) ppm with ^{183}W satellites, (see ESI† for spectra) the result of four inequivalent phosphorus environments expected for **17**. The IR spectrum confirmed the *cis* geometry by the presence of two ν_{CO} bands of nearly equal intensity at 1837 and 1773 cm^{-1}.

Conclusions

Molybdenum and tungsten bis(dinitrogen) complexes bearing pendant amines have been synthesized and isolated in low to moderate yields. Compared to the reductive synthesis of non-pendant amine containing $Mo(N_2)_2$ dinitrogen complexes, the preparation of $Mo(N_2)_2(PNP)_2$ compounds is sensitive to the nature of the Mo starting material. *Cis* and *trans* isomers of Mo bis(dinitrogen) complexes were isolated with ethyl-substituted PNP ligands. The synthesis of $W(N_2)_2$ complexes containing one or two PNP ligands was accomplished by following known synthetic procedures. These complexes have been characterized by NMR and IR spectroscopy, X-ray crystallography and cyclic voltammetry. Based on X-ray data, the complexes are found to activate dinitrogen to a similar degree as analogous complexes without pendant amines. A comparison of ν_{NN} IR stretches and M–N and N–N bond distances between Mo and W PNP complexes indicates stronger $M–N_2$ coordination and more dinitrogen bond activation for tungsten complexes *versus* similar molybdenum complexes, suggesting that tungsten complexes may be better candidates for nitrogen reduction when comparing the molecules examined in this report. In addition, cyclic voltammetry indicates that the incorporation of the pendant amines affects the reversibility of the $M^{II/I}$ couple in the dinitrogen complexes, likely from loss of N_2 facilitated by the pendant amine groups. The addition of CO to selected dinitrogen PNP complexes affords Mo and W dicarbonyl complexes. The reactivity of these dinitrogen complexes with acids is being examined to understand the role of the pendant amine upon protonation and how their presence will affect the intermediates formed during the reduction of dinitrogen.

Experimental

General

Synthesis and materials. All synthetic procedures were performed under an atmosphere of N_2 using standard Schlenk or glovebox techniques. Unless described otherwise, all reagents were purchased from commercial sources and were used as received. Solvents were dried by passage through activated alumina in an Innovative Technology, Inc., PureSolv solvent purification system. Isotopically labelled gases (^{13}CO, $^{15}N_2$) were purchased and used as received from Cambridge Isotope Laboratories. Deuterated THF, toluene, and benzene were purchased from Cambridge Isotope Laboratories, dried over NaK and vacuum transferred before use. Tungsten hexachloride, triphenylphosphine, diphenylphosphine, diethylphosphine, dicyclohexylphosphine, and 1,2-bis(diphenylphosphino)ethane, were purchased from Strem Chemicals, Inc. Magnesium powder, zinc flakes, paraformaldehyde (95%), benzylamine (95%), methylamine in ethanol (33% wt), bromine, 1,3-bis(diphenylphosphino)propane (dppp), and molybdenum hexacarbonyl were purchased from Sigma-Aldrich. Triethylamine was purchased from Alfa-Aesar and distilled over CaH_2 before use. Ferrocene (Aldrich) was sublimed under vacuum before use. $MoBr_3(THF)_3$,[35] **10**,[11] $WCl_4(PPh_3)_2$,[22b] $P^{Ph}N^{Ph}P^{Ph}$,[36] and tetrabutylammonium tetrakis(pentafluorophenyl)borate[37] were synthesized according to literature preparations.

General procedures. NMR spectra were recorded on a Varian 500 MHz Inova or NMR S system unless otherwise indicated. ^{1}H and ^{13}C chemical shifts are referenced to residual protio impurity in deuterated solvent. ^{31}P chemical shifts are proton decoupled unless otherwise noted and referenced to H_3PO_4 as an external reference. ^{15}N NMR chemical shifts were externally referenced to NH_4Cl ($\delta = -341$) relative to CH_3NO_2 ($\delta = 0$). Infrared spectra were recorded on a Thermo Scientific Nicolet iS10 FT-IR spectrometer at ambient temperature and under a purge stream of nitrogen gas. Solid-state FT-IR samples were prepared as KBr pellets. Elemental analysis was performed by Atlantic Microlabs, Norcross, GA. Cyclic voltammetry was performed in a Vacuum Atmospheres Nexus II glovebox under an N_2 atmosphere using a CH Instruments model 620D or 660C potentiostat in THF using 0.2 M tetrabutylammonium tetrakis (pentafluorophenyl)borate as the supporting electrolyte. Measurements were performed using standard three-electrode cell containing a 1 mm PEEK-encased glassy carbon, Cypress Systems EE040, a 3 mm glassy carbon rod (Alfa) as the counter electrode, and a silver wire suspended in electrolyte solution and separated from the analyte solution by a Vycor frit (CH Instruments 112) as the pseudoreference electrode. Prior to the acquisition of each voltammogram, the working electrode was polished using 0.1 µm γ-alumina (BAS CF-1050), and rinsed with THF. Ferrocene or decamethylferrocene (−0.53 V *vs.* $Cp_2Fe^{+/0}$ in THF) was used as an internal reference. All potentials are reported *versus* the ferrocenium–ferrocene couple at 0.0 V and all cyclic voltammograms are collected by first scanning potential in the positive direction.

Typical procedure for synthesis of $P^RN^{Me}P^R$ (R = Ph, Cy, and Et) ligands. To a 50 mL Schlenk flask paraformaldehyde (0.34 g, 11 mmol) and ethanol was loaded and degassed by cycling under vacuum and N_2. The phosphine (11 mmol) was syringed in and the resulting mixture stirred at room temperature for 0.5 h. Methylamine in ethanol (33 wt% in EtOH, 0.60 mL, 5.6 mmol) and triethylamine (1.0 mL) were syringed in and stirred for an additional 3 h at room temperature (50 °C for R = Cy) before removing solvent[38] and volatiles under vacuum to give clear oils or white solids in 70–84% yields for $P^{Et}N^{Me}P^{Et}$,[13b] 81% yield for $P^{Ph}N^{Me}P^{Ph}$,[11] and 97% yield for $P^{Cy}N^{Me}P^{Cy}$.[39]

$P^{Cy}N^{Bn}P^{Cy}$. To a 50 mL Schlenk flask, paraformaldehyde was loaded (0.34 g, 11 mmol) and flushed with N_2 before adding 20 mL anhydrous toluene. Dicylcohexylphosphine (2.2 mL, 11 mmol) was added followed by benzylamine (0.60 mL, 5.6 mmol). The reaction was stirred at 65 °C for 14 h before removing solvent under vacuum to give a clear, viscous oil. Yield (2.24 g, 4.2 mmol, 76%). ^{1}H NMR (THF-d_8, 500 MHz): δ = 7.1–7.0 (m, 5H, $NCH_2C_6H_5$); 3.63 (s, 2H, NCH_2Ph); 2.61 (s, 4H, PCH_2N); 1.7–0.9 (m, 44H, PC_6H_{11}). ^{13}C{^{1}H} NMR

(THF-d$_8$, 125 MHz): δ = 140.9, 130.7, 128.7, 127.6, 62.4, 53.4, 33.8, 30.6, 27.9, 26.4. ^{31}P{^{1}H} NMR (THF): δ = – 16.97 (s).

P^{Et}N^{Bn}P^{Et}. A reaction flask was charged with 2 mL (1.6 g, 18 mmol) diethylphosphine, (0.34 g, 11 mmol) paraformaldehyde and (0.16 g, 5.5 mmol) benzylamine, all dissolved in oxygen free ethanol. The reaction was heated at 70 °C for 2 h. Volatile materials were removed under reduced pressure affording a colorless, viscous oil in 84% yield (2.3 g, 7.6 mmol). ^{1}H NMR (THF-d$_8$): δ = 7.33–7.12 (m, 5H, Ph *H*): 3.79 (s, 2H NC*H*$_2$Ph); 2.74 (m, 4H, PC*H*$_2$N), 1.40–1.29 (m, 8H, PC*H*$_2$CH$_3$), 1.01 (dt, 12H, J_t = 7.4, J_d = 13.9 Hz, PCH$_2$C*H*$_3$). ^{13}C{^{1}H} NMR (C$_6$D$_6$, 125 MHz): δ = 140.3, 130.0 128.3, 127.5, 62.1, 57.3, 19.0, 10.5. ^{31}P{^{1}H} NMR (THF-d$_8$): δ = – 33.0 (s).

P^{Ph}N^{Bn}P^{Ph}. A reaction flask was charged with (2.5 g, 11 mmol) diphenylhydroxymethylphosphine and (0.16 g, 5.5 mmol) benzylamine, dissolved in oxygen free acetonitrile. The reaction was heated at 70 °C for 2 h. Volatile materials were removed under reduced pressure affording a colorless, viscous oil in 92% yield (2.6 g, 5.1 mmol). ^{1}H NMR (THF-d$_8$): δ = 7.38–7.04 (m, 25H, Ph-H): 4.01 (s, 2H NC*H*$_2$Ph); 3.56 (d, 4H, J_{H-P} = 3.1 Hz, PC*H*$_2$N). ^{13}C{^{1}H} NMR (C$_6$D$_6$, 125 MHz): δ = 139.1, 139.0, 134.0, 133.8, 130.1, 129.0, 128.9, 127.6, 61.4, 59.1. ^{31}P{^{1}H} NMR (THF-d$_8$): δ = – 27.9 (s).

Synthesis of molybdenum bromide complexes

MoBr$_3$(THF)$_3$. The preparation by Poli[35] was modified by reducing the temperature for the second bromine addition to −10 °C (ice–salt bath). The reaction was stirred at −10 °C for 4 h or until visible gas evolution has ceased.

MoBr$_2$(P^{Et}N^{Bn}P^{Et})$_2$ (1). Following the procedure from above using 0.225 g of MoBr$_3$(THF)$_3$, the reaction turned bright green and an orange precipitate was observed. Yield (0.075 g, 0.085 mmol, 21%) ^{1}H NMR (CD$_2$Cl$_2$): δ 9.63 (br), 8.66 (d, J = 7.1 Hz), 7.82 (m), 6.55 (s), −5.49 (br), −17.39 (br), −17.76 (br). ^{31}P{^{1}H} NMR: no signal in a range of −500 ppm to +500 ppm. Anal. Calcd for C$_{34}$H$_{62}$MoBr$_2$N$_2$P$_4$: %C, 46.48; %H, 7.11: %N, 3.19. Found: %C, 45.10; %H, 6.87; %N, 3.13.[40]

MoBr$_2$(P^{Ph}N^{Me}P^{Ph})$_2$ (3). Following the procedure from above using 0.25 g of MoBr$_3$(THF)$_3$. Yield (0.40 g, 0.36 mmol, 78%) ^{1}H NMR (CD$_2$Cl$_2$): δ 13.40 (br), 11.39 (br), 10.74 (br), 10.45 (br), 6.84 (br), 4.69 (br), −4.87 (br), −29.57 (br). ^{31}P{^{1}H} NMR: no signal in a range of −500 ppm to +500 ppm. Anal. Calcd for C$_{54}$H$_{54}$Br$_2$MoN$_2$P$_4$: %C, 58.39; %H, 4.90; %N, 2.52. Found: %C, 57.92; %H, 4.72; %N, 2.43.

MoBr$_2$(P^{Ph}N^{Bn}P^{Ph})$_2$ (4). MoBr$_3$(THF)$_3$ (0.25 g, 0.46 mmol) and P^{Ph}N^{Bn}P^{Ph} (0.46 g, 0.90 mmol) were dissolved in 40 mL of THF. Zinc flakes (0.093 g, 1.4 mmol) were added and the reaction was stirred for 19 h resulting in a color change to yellow–brown with a yellow precipitate. The precipitate was isolated on a medium porosity frit. An additional crop can be collected by reducing the volume of the mother liquor (~5 mL) and storing at −35 °C. Yield (0.46 g, 0.37 mmol, 80%) ^{1}H NMR (CD$_2$Cl$_2$): δ 13.28 (br), 11.40 (br), 10.76 (br), 8.01 (m), 7.54 (m), 7.05 (m), 6.76 (m), 4.68 (br), −4.38 (br), −30.63 (br). ^{31}P{^{1}H} NMR: no signal in a range of −500 ppm to +500 ppm. Anal. Calcd for C$_{66}$H$_{62}$Br$_2$MoN$_2$P$_4$: %C, 62.77; %H, 4.95; %N, 2.22. Found: %C, 64.77; %H, 5.13; %N, 2.20.[40]

Synthesis of *cis* and *trans*-[Mo(N$_2$)$_2$(PNP)$_2$] complexes

One pot method

***cis*-[Mo(N$_2$)$_2$(P^{Et}N^{Bn}P^{Et})$_2$] (*cis*-5).** MoBr$_3$(THF)$_3$ (0.225 g, 0.41 mmol), P^{Et}N^{Bn}P^{Et} ligand, (0.25 g, 0.82 mmol), and Mg powder (0.58 g, 24 mmol) was stirred in 50 mL THF in a 100 mL round bottom flask. After 1.5 h, the yellow solution changed to yellow–green, which slowly turned dark orange–brown within 1 h. The reaction mixture was filtered through a medium porosity frit with a Celite pad (0.25 inch), and then the solution was concentrated *in vacuo* and placed in a −35 °C freezer overnight to afford an orange solid in a 17 : 3 ratio of *cis*–*trans* isomers. ^{1}H NMR (THF-d$_8$): δ 7.29 s, 4H, Ph *H*), 7.28 (d, 4H, J = 3 Hz, Ph *H*), 7.21 (m, 2H, Ph *H*), 3.54 (d, 2H, J = 12.5 Hz, PhC*H*$_2$N), 3.46 (d, 2H, J = 12.5 Hz, PhC*H*$_2$N), 3.24 (m, 2H, PC*H*$_2$N), 3.19 (m, 2H, PC*H*$_2$N), 2.29 (m, 2H, PC*H*$_2$N), 2.24 (m, 2H, PC*H*$_2$N), 2.19 (m, 2H, PC*H*$_2$CH$_3$), 2.02 (m, 2H, PC*H*$_2$CH$_3$), 1.99 (m, 2H, PC*H*$_2$CH$_3$), 1.65 (m, 2H, PC*H*$_2$CH$_3$), 1.56 (m, 2H, PC*H*$_2$CH$_3$), 1.46 (m, 4H, PC*H*$_2$CH$_3$), 1.35 (m, 2H, PC*H*$_2$CH$_3$), 1.01 (m, 12H, PCH$_2$C*H*$_3$), 0.92 (m, 12H, PCH$_2$C*H*$_3$). ^{31}P{^{1}H} NMR (THF-d$_8$): δ 15.9(t), 12.5(t): AA′BB′, splitting 24 Hz. IR (KBr, ν_{NN}, cm^{-1}): 2006 (w, sym), 1945 (w, asym).

***trans*-[Mo(N$_2$)$_2$(P^{Et}N^{Bn}P^{Et})$_2$] (*trans*-5).** Yield (0.23 g, 0.30 mmol, 64%) ^{1}H NMR (THF-d$_8$): δ 7.37–7.33 (m, 4H, Ph *H*), 7.31–7.27 (m, 4H, Ph *H*), 7.24–7.19 (m, 2H, Ph *H*), 3.51 (s, 4H, C*H*$_2$Ph), 2.80 (s, 8H, PC*H*$_2$N), 1.94–1.82 (m, 8H, PC*H*$_2$CH$_3$), 1.80–1.69 (m, 8H, PC*H*$_2$CH$_3$), 1.03–0.93 (m, 24H, CH$_2$C*H*$_3$). ^{31}P{^{1}H} NMR (THF-d$_8$): δ 12.4 (s). IR (KBr, ν_{NN}, cm^{-1}): 2006 (w, sym), 1937 (s, asym). Anal. Calcd for C$_{34}$H$_{62}$MoN$_6$P$_4$: %C, 52.71; %H, 8.07; %N, 10.85. Found: %C, 51.04; %H, 8.02; %N, 10.05.

***cis*-[Mo(N$_2$)$_2$(P^{Et}N^{Me}P^{Et})$_2$] (*cis*-6).** Following the procedure from above, a 14 : 6 ratio of *cis*–*trans* isomers was obtained. ^{1}H NMR (THF-d$_8$): δ 3.10 (m, 2H, PC*H*$_2$N), 2.99 (m, 2H, PC*H*$_2$N), 2.30 (s, 6H, NC*H*$_3$), 2.26 (m, 2H, PC*H*$_2$N), 2.23 (m, 2H, PC*H*$_2$CH$_3$), 2.12 (m, 2H, PC*H*$_2$N), 2.08 (m, 2H, PC*H*$_2$CH$_3$), 1.94 (m, 2H PC*H*$_2$CH$_3$), 1.82 (m, 4H, PC*H*$_2$CH$_3$), 1.45 (m, 4H, PC*H*$_2$CH$_3$), 1.42 (m, 2H, PC*H*$_2$CH$_3$), 1.13 (m, 12H, PCH$_2$C*H*$_3$), 1.06 (m, 6H, PCH$_2$C*H*$_3$), 1.00 (m, 6H, PCH$_2$C*H*$_3$). ^{31}P{^{1}H} NMR (THF-d$_8$): δ 15.2(t), 12.8(t): AA′BB′, splitting 24 Hz. IR (KBr, ν_{NN}, cm^{-1}): 2007 (s, sym) 1940 (s, asym).

Note: the orange microcrystalline solid of *cis*-[Mo(N$_2$)$_2$(PNP)$_2$] complexes turns brown over a period of approximately 10 days, and no longer contain ν_{NN} bands by IR.

***trans*-[Mo(N$_2$)$_2$(P^{Et}N^{Me}P^{Et})$_2$] (*trans*-6).** Following the procedure from above, the *trans* isomer is prepared by stirring the reaction mixture for 22 h. The solvent was removed and the *trans* isomer was extracted with diethyl ether to give 85% *trans* isomer. Yield (0.28 g, 0.45 mmol, 71%). ^{1}H NMR (300 MHz, THF-d$_8$): δ 2.69 (s, 8H, PC*H*$_2$N), 2.31 (s, 6H, NC*H*$_3$), 1.79–1.87 (m, 8H, PC*H*$_2$CH$_3$), 1.87–1.75 (m, 8H, PC*H*$_2$CH$_3$), 1.19–1.07 (m, 24H, PCH$_2$C*H*$_3$). ^{31}P{^{1}H} NMR (THF-d$_8$): δ 12.0 (s). IR

(KBr, ν_{NN}, cm^{-1}): 1937 (s, asym). Anal. Calcd for $C_{22}H_{54}MoN_6P_4$: %C, 42.44; %H, 8.74; %N, 13.50. Found: %C, 42.84; %H, 8.76; %N, 13.00.

Synthesis of *trans*-bis(dinitrogen) complex: stepwise method

***trans*-[Mo(N_2)$_2$($P^{Ph}N^{Me}P^{Ph}$)$_2$] (7-Mo).** $MoBr_2(P^{Ph}N^{Me}P^{Ph})_2$ (0.175 g, 0.157 mmol) was suspended in 75 mL THF with Mg powder (0.075 g, 2.25 mmol). The reaction was stirred for 24 h. The reaction mixture was filtered through Celite and the mother liquor concentrated *in vacuo* to ~10 mL. The solution was stored at −35 °C for 18 h affording a dark yellow microcrystalline solid that was dried under vacuum. Yield (0.024 g, 0.023 mmol, 15%). ^{1}H NMR (THF-d$_8$): δ 7.13 (t, 8H, J = 7.2 Hz, Ph-H), 7.03 (m, 16H, Ph-H), 6.98 (t, 16H, J = 7.2 Hz, Ph-H), 3.20 (s, 8H, PCH_2N), 2.09 (s, 6H, NCH_3). $^{31}P\{^1H\}$ NMR (THF-d$_8$): δ 25.3 (s). IR (KBr, ν_{NN}, cm^{-1}): 1955 (s, asym). Anal. Calcd for $C_{54}H_{54}MoN_6P_4$: %C, 64.41; %H, 5.41; %N, 8.35. Found: %C, 64.15; %H, 5.30; %N, 7.99.

***trans*-[Mo(N_2)$_2$($P^{Ph}N^{Bn}P^{Ph}$)$_2$] (8).** Following the procedure from above using (0.20 g, 0.16) $MoBr_2(P^{Ph}N^{Bn}P^{Ph})_2$. Yield (0.084 g, 0.072 mmol, 40%). ^{1}H NMR (THF-d$_8$): δ 7.14 (m, 8H, Ph *H*), 7.04–6.90 (m, 38H, Ph *H*), 6.67 (m, 4H, Ph *H*), 3.31 (s, 4H, NCH_2Ph), 2.29 (s, 8H, NCH_2Ph). $^{31}P\{^1H\}$ NMR (THF-d$_8$): δ 27.9 (s). IR (KBr, ν_{NN}, cm^{-1}): 1954 (s, asym).

Synthesis of *cis* and *trans* $Mo(CO)_2(PNP)_2$

Beginning with the complex **7-Mo**, 0.05g was dissolved in THF-d$_8$ in a septum capped NMR tube, the N_2 atmosphere was purged by bubbling an atmosphere of CO through the reaction mixture for ~2 min, and then periodically mixed by a vortex mixer over the course of 24 h, until all bis(dinitrogen) complex had been consumed. The products were monitored by NMR, showing initial formation of *trans* dicarbonyl. Over the course of 8 h the *trans* isomer converts to the *cis* isomer. In the case of the ^{13}C labelled CO, a J. Young NMR tube with a Teflon valve was used to evacuate the headspace of the tube (freeze, pump, thaw three times), and finally dose in the isotopically labelled gas.

***cis*-[Mo(CO)$_2$($P^{Et}N^{Bn}P^{Et}$)$_2$].** $^{31}P\{^1H\}$ NMR (THF-d$_8$): δ 15.4 (t), 3.1(t): AA′BB′, splitting 30 Hz. IR (THF, ν_{CO}, cm^{-1}): 1837 (s), 1768 (s).

***cis*-[Mo(^{13}CO)$_2$($P^{Et}N^{Bn}P^{Et}$)$_2$].** δ 15.4 (tt, J_t = 10.8 Hz, AA′BB′ splitting 30 Hz), 3.1 (td, J_d = 16.6 Hz, AA′BB′ splitting 30 Hz). IR (THF, ν_{CO}, cm^{-1}): 1802 (s, sym), 1742 (s, asym).

***trans*-[Mo(CO)$_2$($P^{Ph}N^{Me}P^{Ph}$)$_2$].** $^{31}P\{^1H\}$ NMR (THF-d$_8$): δ 31.4 (s). IR (KBr, ν_{CO}, cm^{-1}): 1805 (s, asym).

***trans*-[Mo(^{13}CO)$_2$($P^{Ph}N^{Me}P^{Ph}$)$_2$].** $^{31}P\{^1H\}$ NMR (THF-d$_8$): δ 31.4 (t, J = 9.2 Hz). IR (THF, ν_{CO}, cm^{-1}): 1885 (s, asym).

***cis*-[Mo(CO)$_2$($P^{Ph}N^{Me}P^{Ph}$)$_2$].** $^{31}P\{^1H\}$ NMR (300 MHz, THF-d$_8$): δ $^{31}P\{^1H\}$ NMR (THF-d$_8$): δ 27.5(t), 12.3(t): AA′BB′, splitting 12 Hz. IR (THF, ν_{CO}, cm^{-1}): 1846 (s, sym), 1781 (s, asym).

***cis*-[Mo(^{13}CO)$_2$($P^{Ph}N^{Me}P^{Ph}$)$_2$].** $^{31}P\{^1H\}$ NMR (THF-d$_8$): δ 27.5 (m), 12.3 (m). IR (THF, ν_{CO}, cm^{-1}): 1834 (s, sym), 1772 (s, asym).

Synthesis of tungsten complexes

***trans*-[W(N_2)$_2$(dppe)($P^{Et}N^{Me}P^{Et}$)] (9).** To a 100 mL round-bottom flask, loaded $P^{Et}N^{Me}P^{Et}$ (0.062 g, 0.26 mmol), WCl_4(dppe) (0.187 g, 0.26 mmol), Mg powder (0.317 g, 13.0 mmol), and 30 mL of THF and stirred vigorously under N_2 for 64 h. The reaction mixture was filtered and dried *in vacuo* affording and extracted with pentane to obtain a red–orange solution. The material was cooled to −35 °C in THF to obtain red-orange crystals. Yield (0.037 g, 0.042 mmol, 16%). ^{1}H NMR (THF-d$_8$): δ 7.49 (t, 8H, J = 8.0 Hz, Ph*H*), 7.30 (t, 8H, Ph*H*), 7.24 (m, 4H, Ph*H*), 2.81 (s, 4H, PCH_2N), 2.26 (s, 3H, NCH_3), 2.24–2.11 (m, 4H, PCH_2CH_2P), 1.88–1.78 (m, 8H, PCH_2CH_3), 0.75 (t, 6H, J = 7.7 Hz, PCH_2CH_3), 0.72 (t, 6H, J = 7.7 Hz, PCH_2CH_3). $^{31}P\{^1H\}$ NMR (THF-d$_8$): δ 45.6 (m with J_{P-W} = 319 Hz ^{183}W satellites, 2P), −13.2 (m with J_{P-W} = 302 Hz ^{183}W satellites, 2P). IR (KBr, ν_{NN}, cm^{-1}): 1990 (w, sym), 1921 (s, asym). Anal. Calcd for $C_{37}H_{51}N_5P_4W$: %C, 50.87; %H, 5.88; %N, 8.02. Found: %C, 51.32, %H, 5.85; %N, 7.79.

***trans*-[W($^{15}N_2$)$_2$(dppe)($P^{Et}N^{Me}P^{Et}$)] (9-^{15}N).** Following the procedure from *trans*-[W(N_2)$_2$(dppe)($P^{Et}N^{Me}P^{Et}$)$_2$] using labelled $^{15}N_2$ gas. The reaction work-up and subsequent handling were performed under Ar. $^{15}N\{^1H\}$ NMR (THF-d$_8$): δ −46 (d, J_{N-N} = 2 Hz, W–N≡*N*), −58 (m, J_{N-W} = 51 Hz ^{183}W satellites, W–*N*≡N). IR (KBr, ν_{NN}, cm^{-1}): 1859 (s, asym).

***trans*-[W(N_2)$_2$(dppe)($P^{Et}N^{Bn}P^{Et}$)] (11).** Following the procedure from *trans*-[W(N_2)$_2$(dppe)($P^{Et}N^{Me}P^{Et}$)] using $P^{Et}N^{Bn}P^{Et}$ in place of $P^{Et}N^{Me}P^{Et}$, *trans*-[W(N_2)$_2$(dppe)($P^{Et}N^{Bn}P^{Et}$)] was synthesized. Due to impurities, full characterization is not obtainable. $^{31}P\{^1H\}$ NMR (THF-d$_8$): δ 45.5 (m with J_{P-W} = 319 Hz ^{183}W satellites, 2P), −14.0 (m with J_{P-W} = 303 Hz ^{183}W satellites, 2P). IR (KBr, ν_{NN}, cm^{-1}): 1990 (w, sym), 1922 (s, asym).

***trans*-[W(N_2)$_2$(dppe)(dppp)] (13).** Dppp ligand (0.94 g, 2.33 mmol), WCl_4,(dppe) (1.64 g, 2.27 mmol), Mg powder (1.00 g, 82.3 mmol), and 50 mL of THF were combined and stirred vigorously for 44 h under N_2. The reaction was filtered and concentrated *in vacuo* affording a red–orange solid. Yield (0.121 g, 0.115 mmol, 5%) product containing 15% *trans*-[W(N_2)$_2$(dppe)$_2$] contaminant. ^{1}H NMR (THF-d$_8$): δ 2.70 (bs, 4H, PCH_2), 2.01 (bs, 4H, PCH_2), 1.89 (m, 2H, $(PCH_2)_2CH_2$). IR (KBr, ν_{NN}, cm^{-1}): 1995 (w, sym), 1917 (s, asym). $^{31}P\{^1H\}$ NMR (THF-d$_8$): δ 44.2 (m with J_{P-W} = 311 Hz ^{183}W satellites), 1.5 (m with J_{P-W} = 314 Hz ^{183}W satellites).

***trans*-[W(N_2)$_2$($P^{Ph}N^{Me}P^{Ph}$)$_2$] (7-W).** $P^{Ph}N^{Me}P^{Ph}$ (1.01 g, 2.37 mmol), WCl_4,$(PPh_3)_2$ (1.02 g, 1.20 mmol), Mg powder (2.91 g, 120 mmol), and 70 mL of THF were added and stirred vigorously for 18 h under N_2. The reaction mixture was filtered and concentrated *in vacuo* and cooled to −35 °C crashing out a light orange solid which was dissolved solid in minimal toluene and cooled to −35 °C to obtain red–orange crystals. Yield (0.12 g, 0.11 mmol, 9%) ^{1}H NMR (THF-d$_8$): δ 7.12 (t, 8H,

J = 7.3 Hz, Ph H), 7.06–6.95 (m, 32H, Ph H), 3.26 (s, 8H, PCH_2N), 2.06 (s, 6H, NCH_3). $^{31}P\{^1H\}$ NMR (THF-d_8): δ −3.1 (s with $J_{P–W}$ = 308 Hz ^{183}W satellites). IR (KBr, ν_{NN}, cm^{-1}): 2027 (w, sym), 1925 (s, asym). Anal. Calcd for $C_{54}H_{54}N_6P_4W \cdot C_4H_8O$: C, 59.70; H, 5.36; N, 7.20. Found: C, 60.22; H, 5.35; N, 7.07.

***trans*-[W($^{15}N_2$)$_2$($P^{Ph}N^{Me}P^{Ph}$)$_2$] (7-W$^{15}N_2$).** Following the procedure from *trans*-[W(N_2)$_2$($P^{Ph}N^{Me}P^{Ph}$)$_2$] using labelled $^{15}N_2$ gas. The reaction work-up and subsequent handling were performed under Ar. $^{15}N\{^1H\}$ NMR (THF-d_8): δ −51 (d, $J_{N–N}$ = 5 Hz, W–N≡N), −62 (d with $J_{N–W}$ = 51 Hz ^{183}W satellites, $J_{N–N}$ = 5 Hz, W–N≡N). IR (KBr, ν_{NN}, cm^{-1}): 1959 (w, sym), 1867 (s, asym).

***cis*-[W(N_2)$_2$($P^{Et}N^{Me}P^{Et}$)$_2$] (*cis*-12).** $P^{Et}N^{Me}P^{Et}$ (0.051 g, 0.22 mmol) and $WCl_4(PPh_3)_2$ (0.093 g, 0.11 mmol) were combined in 30 mL THF and stirred for 3 min. Mg powder (0.771 g, 31.7 mmol) was added and the reaction was stirred for 23 h before being filtered and dried *in vacuo* to afford a yellow oil. Due to the high solubility in a variety of organic solvents, the complex was not obtained pure. ^1H NMR (THF-d_8): δ 3.18 (m, 2H, PCH_2N), 3.12 (m, 2H, PCH_2N), 2.36 (m, 2H, PCH_2CH_3), 2.28 (m, 2H, PCH_2N), 2.26 (s, 6H, NCH_3), 2.20 (m, 2H, PCH_2CH_3), 2.14 (m, 2H, PCH_2N), 2.10 (m, 2H PCH_2CH_3), 1.94 (m, 4H, PCH_2CH_3), 1.53 (m, 4H, PCH_2CH_3), 1.43 (m, 2H, PCH_2CH_3), 1.12 (m, 12H, PCH_2CH_3), 1.04 (m, 6H, PCH_2CH_3), 0.98 (m, 6H, PCH_2CH_3). $^{31}P\{^1H\}$ NMR (THF-d_8): δ −12.1 (t with ^{183}W satellites $J_{P–W}$ = 296 Hz, 2P), −13.7 (t with ^{183}W satellites $J_{P–W}$ = 304 Hz, 2P): AA′BB′, splitting 15 Hz. IR (KBr, ν_{NN}, cm^{-1}): 1981 (s, sym), 1916 (s, asym).

***trans*-[W(N_2)$_2$($P^{Et}N^{Me}P^{Et}$)$_2$] (*trans*-12).** Following the procedure from *cis*-[W(N_2)$_2$($P^{Et}N^{Me}P^{Et}$)$_2$] (*cis*-**12**), *trans*-**12** was produced as a minor product. $^{31}P\{^1H\}$ NMR (THF-d_8): δ −15.2 (s). IR (KBr, ν_{NN}, cm^{-1}): 1942 (s, asym).

***trans*-[W(N_2)$_2$(dppp)$_2$] (14).** Following the procedure from *trans*-[W(N_2)$_2$($P^{Ph}N^{Me}P^{Ph}$)$_2$] using dppp in place of $P^{Ph}N^{Me}P^{Ph}$, *trans*-[W(N_2)$_2$(dppp)$_2$] was synthesized. Due to the complex product mixture and small relative quantity of *trans*-[W(N_2)$_2$(dppp)$_2$] to other products, full characterization is not obtainable. See ESI† for the ^{31}P NMR spectrum of the product mixture. ^1H NMR (C_6D_6): δ 7.38 (m, 16H, Ph H), 7.05 (m, 24H, Ph H), 2.04 (m, 8H, PCH_2), 1.66 (m, 4H, $P(CH_2)_2CH_2$). $^{31}P\{^1H\}$ NMR (C_6D_6): δ −3.5 (s with $J_{P–W}$ = 307 Hz ^{183}W satellites). IR (KBr, ν_{NN}, cm^{-1}): 1912 (s, asym).

***cis*-[W(CO)$_2$(dppe)($P^{Et}N^{Me}P^{Et}$)$_2$] (17).** $^{31}P\{^1H\}$ NMR (THF-d_8): δ 46.8 (ddd, 1P, $J_{P–P}$ = 74.3, 18.5, 8.5), 39.9 (ddd, 1P, $J_{P–P}$ = 18.5, 8.5, 18.5), −11.2 (ddd, 1P, $J_{P–P}$ = 74.3, 18.5, 27.9), −24.5 (ddd, 1P, $J_{P–P}$ = 18.5, 27.9, 18.5). IR (KBr, ν_{CO}, cm^{-1}): 1837 (s, sym), 1773 (s, asym).

X-Ray diffraction studies. Single crystals of *trans*-[W(N_2)$_2$(dppe)($P^{Et}N^{Me}P^{Et}$)], *trans*-[W(N_2)$_2$($P^{Et}N^{Me}P^{Et}$)$_2$], *trans*-[W(N_2)$_2$(dppe)($P^{Ph}N^{Me}P^{Ph}$)], *trans*-[W(N_2)$_2$($P^{Ph}N^{Me}P^{Ph}$)$_2$], and *trans*-[W(N_2)$_2$($PMePh_2$)$_4$] and all of the *trans* isomers of *trans*-[Mo(N_2)$_2$($P^{Et}N^{Bn}P^{Et}$)$_2$], *trans*-[Mo(N_2)$_2$($P^{Ph}N^{Me}P^{Ph}$)$_2$], *trans*-[$MoBr_2$($P^{Et}N^{Bn}P^{Et}$)$_2$], *trans*-[$MoBr_2$($P^{Ph}N^{Bn}P^{Ph}$)$_2$], *trans*-[Mo(N_2)$_2$($P^{Et}N^{Me}P^{Et}$)$_2$], and *cis*-[Mo(N_2)$_2$($P^{Et}N^{Me}P^{Et}$)$_2$] were mounted using NVH immersion oil onto a nylon fiber and cooled to the data collection temperature of 100(2) K. Data were collected on a Brüker-AXS Kappa APEX II CCD diffractometer with 0.71073 Å Mo-Kα radiation. Unit cell parameters were obtained from 90 data frames, 0.3° Φ, from three different sections of the Ewald sphere. The data-set was treated with SADABS absorption corrections based on redundant multi-scan data. All non-hydrogen atoms were refined with anisotropic displacement parameters and were treated as idealized contributions. Details for solution and refinement are provided in the ESI† section.

Acknowledgements

This material is based upon work supported as part of the Center for Molecular Electrocatalysis, an Energy Frontier Research Center funded by the U.S. Department of Energy, Office of Science, Office of Basic Energy Sciences, under FWP 56073. Pacific Northwest National Laboratory is operated by Battelle for DOE.

Notes and references

1 (*a*) R. Schlögl, *Angew. Chem., Int. Ed.*, 2003, **42**, 2004; (*b*) V. Smil, *Enriching the Earth: Fritz Haber, Carl Bosch, and the Transformation of World Food Production*, MIT Press, Cambridge, 2001.

2 (*a*) J. B. Howard and D. C. Rees, *Chem. Rev.*, 1996, **96**, 2965; (*b*) B. K. Burgess and D. J. Lowe, *Chem. Rev.*, 1996, **96**, 2983.

3 B. E. Smith, *Science*, 2002, **297**, 1654.

4 (*a*) M. D. Fryzuk and S. A. Johnson, *Coord. Chem. Rev.*, 2000, **200–202**, 379; (*b*) R. L. Richards, *Coord. Chem. Rev.*, 1996, **154**, 83; (*c*) A. D. Allen and C. V. Senoff, *J. Chem. Soc. Chem. Commun.*, 1965, 621.

5 (*a*) K. Arashiba, Y. Miyake and Y. Nishibayashi, *Nat. Chem.*, 2010, **3**, 120; (*b*) D. V. Yandulov and R. R. Schrock, *Inorg. Chem.*, 2005, **44**, 1103; (*c*) D. V. Yandulov and R. R. Schrock, *Science*, 2003, **301**, 76; (*d*) W. W. Weare, X. Dai, M. J. Byrnes, J. M. Chin, R. R. Schrock and P. Müller, *Proc. Natl. Acad. Sci. U. S. A.*, 2006, **103**, 17099; (*e*) R. R. Schrock, *Acc. Chem. Res.*, 2005, **38**, 955.

6 (*a*) J. Chatt, J. R. Dilworth and R. L. Richards, *Chem. Rev.*, 1978, **78**, 589; (*b*) G. J. Leigh, *Acc. Chem. Res.*, 1992, **25**, 177; (*c*) J. Chatt, A. J. Pearman and R. L. Richards, *J. Chem. Soc., Dalton Trans.*, 1976, 1520; (*d*) M. Hidai and Y. Mizobe, *Chem. Rev.*, 1995, **95**, 1115; (*e*) T. Takahashi, Y. Mizobe, M. Sato, Y. Uchida and M. Hidai, *J. Am. Chem. Soc.*, 1980, **102**, 7461; (*f*) J. Chatt, A. J. Pearman and R. L. Richards, *Nature*, 1975, **253**, 39.

7 (*a*) D. L. DuBois and R. M. Bullock, *Eur. J. Inorg. Chem.*, 2011, 1017; (*b*) M. Rakowski DuBois and D. L. DuBois, in *Catalysis Without Precious Metals*, ed. R. M. Bullock, Wiley-VCH, Weinheim, 2010, pp. 165–180; (*c*) M. Rakowski DuBois and D. L. DuBois, *Acc. Chem. Res.*, 2009, **42**, 1974.

8 M. L. Helm, M. Stewart, R. M. Bullock, M. Rakowski DuBois and D. L. DuBois, *Science*, 2011, **333**, 863.

9 T. A. Tronic, M. Rakowski DuBois, W. Kaminsky, M. K. Coggins, T. Liu and J. M. Mayer, *Angew. Chem., Int. Ed.*, 2011, **50**, 10936.

10 M. T. Mock, S. Chen, R. Rousseau, M. J. O'Hagan, W. G. Dougherty, W. S. Kassel, D. L. DuBois and R. M. Bullock, *Chem. Commun.*, 2011, **47**, 12212.

11 G. Stephan, C. Näther, C. Sivasankar and F. Tuczek, *Inorg. Chim. Acta*, 2008, **361**, 1008.

12 G. Stephan, C. Näther and F. Tuczek, *Acta Crystallogr., Sect. E: Struct. Rep. Online*, 2008, **E64**, m629.

13 (*a*) K. D. Welch, W. G. Dougherty, W. S. Kassel, D. L. DuBois and R. M. Bullock, *Organometallics*, 2010, **29**, 4532; (*b*) C. J. Curtis, A. Miedaner, R. F. Ciancanelli, W. W. Ellis, B. C. Noll, M. Rakowski DuBois and D. L. DuBois, *Inorg. Chem.*, 2003, **42**, 216.

14 (*a*) M. Yuki, Y. Miyake and Y. Nishibayashi, *Organometallics*, 2008, **27**, 3947; (*b*) F. Stoffelbach, D. Saurenz and R. Poli, *Eur. J. Inorg. Chem.*, 2001, 2699.

15 The reason for the difference in reactivity between molybdenum chlorides and bromides is not clear but we speculate that the molybdenum chlorides are forming insoluble aggregating during the reduction with PNP ligands.

16 (*a*) T. A. George and M. E. Noble, *Inorg. Chem.*, 1978, **17**, 1678; (*b*) J. R. Dilworth and R. L. Richards, *Inorg. Synth.*, 1980, **20**, 119.

17 N. J. Lazarowych, R. H. Morris and J. M. Ressner, *Inorg. Chem.*, 1986, **25**, 3926.

18 S. A. Best, T. J. Smith and R. A. Walton, *Inorg. Chem.*, 1978, **17**, 99.

19 (*a*) P. A. Agaskar and F. A. Cotton, *Inorg. Chem.*, 1984, **23**, 3383; (*b*) P. A. Agaskar and F. A. Cotton, *Inorg. Chem.*, 1986, **25**, 15.

20 R. J. Butcher and W. J. Jones, *J. Chem. Soc., Faraday Trans.*, 1974, **70**, 560.

21 (*a*) T. A. George, J. R. D. DeBord, B. B. Kaul, C. J. Pickett and D. J. Rose, *Inorg. Chem.*, 1992, **31**, 1295; (*b*) W. Hussain, G. J. Leigh, H. M. Ali, C. J. Pickett and D. A. Rankin, *J. Chem. Soc., Dalton Trans.*, 1984, 1703.

22 (*a*) R. Römer, C. Gradert, A. Bannwarth, G. Peters, C. Näther and F. Tuczek, *Dalton Trans.*, 2011, **40**, 3229; (*b*) J. R. Dilworth and R. L. Richards, *Inorg. Synth.*, 2007, **28**, 3343.

23 The symmetric band for *trans*-$[W(^{15}N_2)_2(dppe)(P^{Et}N^{Me}P^{Et})]$ is obscured by bands due to *trans*-$[W(^{14}N_2)_2(dppe)(P^{Et}N^{Me}P^{Et})]$ and thus could not be accurately measured.

24 A ν_{NN} stretch in the IR spectrum at 1945 cm^{-1} was observed for a tungsten complex synthesized with $P^{Cy}N^{Me}P^{Cy}$: suggesting an N_2 complex was formed. No signals are observed in the $^{31}P\{^1H\}$ NMR spectrum, indicating a paramagnetic species.

25 C. Hu, W. C. Hodgeman and D. W. Bennett, *Inorg. Chem.*, 1996, **35**, 1621.

26 Liquid ammonia is located at −380 ppm in a ^{15}N NMR spectrum referenced to nitromethane (0 ppm).

27 See ESI† for $^{31}P\{^1H\}$ NMR spectrum of product mixture.

28 B. A. MacKay and M. D. Fryzuk, *Chem. Rev.*, 2004, **104**, 385.

29 D. L. DuBois and R. Hoffmann, *Nouv. J. Chem.*, 1977, **1**, 479.

30 R. A. Henderson, *J. Chem. Soc., Dalton Trans.*, 1982, 917.

31 Images of the structures of *trans*-**12** and *trans*-$[WCl_2(P^{Et}N^{Me}P^{Et})_2]$ are available in the ESI† (Fig. S8-9).

32 *cis*-$[WCl_2(depe)_2]$ is reported as private communication by J. Cugny, H.W. Schmalle, and H. Berke (CCDC 248972). The bond distances and angles for *cis*-$[WCl_2(P^{Et}N^{Me}P^{Et})_2]$ are reported in the ESI†.

33 Examination of potentials more negative than −2.0 V was limited by the solvent window for THF stopping at −2.5 to −3.0 V.

34 (*a*) T. J. Chow, C.-Y. Wang, S.-C. Sheu and S.-M. Peng, *J. Organomet. Chem.*, 1986, **311**, 339; (*b*) M. Hidai, K. Tominari and Y. Uchida, *J. Am. Chem. Soc.*, 1972, **94**, 110.

35 B. E. Owens, R. Poli and A. L. Rheingold, *Inorg. Chem.*, 1989, **28**, 1456.

36 A. Balch, M. M. Olmstead and S. P. Rowley, *Inorg. Chim. Acta*, 1990, **168**, 255.

37 R. J. LeSuer and W. E. Geiger, *Angew. Chem., Int. Ed.*, 2000, **39**, 248.

38 Add more methylamine and stir for an additional 3 h if R_2PCH_2OH intermediate is not fully consumed. The R_2PCH_2OH intermediates exhibit singlets in the $^{31}P\{^1H\}$ NMR at −17.2, −17.0, and −12.2 ppm in THF for R = Et, Cy, and Ph, respectively.

39 O. Serindag, R. D. W. Kemmitt, J. Fawcett and D. R. Russell, *Transition Met. Chem.*, 1999, **24**, 486.

40 While the carbon values are slightly off in the combustion analysis in four separate attempts, hydrogen and nitrogen consistently gave acceptable values.